



Radiation Oncology
UNIVERSITY OF TORONTO

welcome to

2021 UTDRO

RESEARCH DAY

UTDRO RESEARCH DAY – TABLE OF CONTENTS

Co-Chair Welcome	1
Program Schedule	2
Poster List	3
Abstracts – Oral	6
Abstracts – Poster	23

UTDRO RESEARCH DAY – THANK YOU

A big thank you to everyone who have helped to organize and run UTDRO Research Day 2021!

CO-CHAIRS

Michael Milosevic, William Tran

COMMITTEE

Andrea McNiven, Ewa Szumacher, Hedi Katalmohseni, Irene Karam, Jennifer Croke, Marianne Koritzinsky, Meghan Ward, Michael Tjong, Olga Pidhirska, Rachel Glicksman, Shane Harding

ABSTRACT REVIEWERS

Adam Gladwish, Alexandra Rink, Anne Koch, Anthony Fyles, Darby Erler, Eric Leung, Ewa Szumacher, Irene Karam, Jean-Pierre Bissonnette, Jeff Winter, Lee Chin, Marianne Koritzinsky, Mark Ruschin, Michael Velec, Mike Milosevic, Renee Korol, Robert Weersink, Shane Harding, William Tran

MODERATORS

Andrea McNiven, Jennifer Croke, Lori Holdings, Shane Harding

EVENT SUPPORT

Catherine Wong, Eileen Brosnan, Olga Pidhirska, Meghan Ward, Tanya Webb

JUDGES

Alex Vitkin, Beibei Zhang, Ben Lok, Brian Liszewski, Catherine Coolens, Darby Erler, Eric Leung, Gerard Morton, Kathy Han, Lee Chin, Marianne Kortzinsky, Mark Ruschin, May Tsao, Michael Velec, Mike Milosevic, Phil Wong, Tim Craig

UTDRO RESEARCH DAY – CO-CHAIR WELCOME

On behalf of the organizing committee, welcome to the University of Toronto, Department of Radiation Oncology (UTDRO) Research Day 2021!

We are excited to showcase the extraordinary work that our trainees in radiation oncology, medical physics, radiotherapy and basic radiation sciences are undertaking in our department. We hope that this program will initiate thoughtful dialogue and synergize new collaborations within the UTDRO clinical and academic community. This meeting is aimed to provide a cross-section of our research accomplishments together and highlight the diverse and innovative work that our trainees have been involved in over the past year.


We also welcome Dr. Anthony Zeitman, MD FASTRO as our keynote speaker. Dr. Zeitman is the Professor of Radiation Oncology at Harvard Medical School and is past-President and Chair of ASTRO. Currently at the Massachusetts General Hospital in Boston, USA, he serves as a program director for the Harvard Radiation Oncology Residency Program and has been a Trustee of the American Board of Radiology.

Since 2011, Dr. Zeitman has been the Editor-in-Chief of the International Journal of Radiation Oncology Biology Physics (Red Journal) helping to chart

its way from traditional scientific journal to a journal of the future! In 2016 he won the ASTRO Gold Medal for his achievements, and we are looking forward to gaining Dr. Zietman's insight into the diverse stories of the radiation oncology team members who create the inspirational cover art for the Red Journal.

Finally, we would like to extend a special thanks to our UTDRO Chair, Dr. Fei-Fei Liu as well all faculty members, and UTDRO staff for their continued support and participation. We hope that you enjoy the program!

Sincerely,



Mike Milosevic, MD, FRCPC
Professor and Vice Chair, Research



William T. Tran, MRT(T), MSCc, PhD
Assistant Professor

UTDRO RESEARCH DAY SCHEDULE

Details: May 5, 2021, 12:00 pm – 3:00 pm

Location: Zoom

Time	Total Length	Main Room	Breakout Room
12:00 PM	5 mins	<i>UTDRO Chair Welcome</i> Fei-Fei Liu, UTDRO Chair	
12:05 PM	5 mins	<i>Opening Remarks and Keynote Introduction</i> William Tran, Program Co-Chair	
12:10 PM	45 mins	<i>Keynote Speaker</i> The Cover Art of the Red Journal: A Reflection on the Creativity of the Radiation Oncology Team Dr. Anthony Zietman, MD, FASTRO	
12:55 PM	10 mins	<i>Break</i>	
01:05 PM	40 mins	Oral Presentations: Section 1 (Moderated by Lori Holden)	Oral Presentations: Section 2 (Moderated by Jennifer Croke)
		1. A Machine Learning Challenge for Prognostic Modelling in Head and Neck Cancer Using Multi-modal Data Michal Kazmierski	5. CNN-based Segmentation of Multiple Needles for Magnetic Resonance-guided Interventions Amanda Aleong
		2. Local control in Tumor-targeted Dose Escalation for Localized Prostate Cancer: A Report on the Target Study Jerusha Padayachee	6. Dosimetric Comparison in Malignant Glioma Patients Clinically Treated on Hybrid Magnetic Resonance Imaging (MRI)-Linac (MRL) versus Conventional Linac Michael H. Wang
		3. A Prognostic Model for Patients with Oligometastatic Disease Treated with Stereotactic Body Radiation Therapy Hanbo Chen	7. Access to Radiotherapy in Ghana: A Geospatial Analysis Aba Scott
		4. Hearing Loss After Radiation and Chemotherapy for Central Nervous System and Head and Neck Tumors in Children Dana Keilty	8. T-DM1 Increases the Risk of SRS-induced Radiation Necrosis in Her2+ Breast Cancer Badr Id Said
1:45 PM	10 mins	Rapid Fire Presentations 1: Posters 1 – 8 (Moderated by Lori Holden)	Rapid Fire Presentations 2: Posters 9 – 16 (Moderated by Jennifer Croke)
1:55 PM	10 mins	<i>Break</i>	

UTDRO RESEARCH DAY SCHEDULE [CON'T]

Details: May 5, 2021, 12:00 pm – 3:00 pm

Location: Zoom

Time	Total Length	Main Room	Breakout Room
2:05 PM	40 mins	Oral Presentations: Section 3 (Moderated by Shane Harding)	Oral Presentations: Section 4 (Moderated by Andrea McNiven)
		9. Hypofractionated Radiotherapy for Breast Cancer: Findings from an International ESTRO-GIRO Survey Melinda Mushonga	13. Quantitative Texture Analysis of Optical Coherence Tomography Images for Early Detection of Tumour Response to Radiotherapy Natalia Demidova
		10. Province-Wide Analysis of Patient Reported Outcomes for Stage IV Non-Small Cell Lung Cancer Michael Tjong	14. Predictive Modeling for Rapid Online Evaluation of Plan Quality During Intraoperative Gynecological Brachytherapy Priscilla Dreyer
		11. A Comparison of Hypofractionated and Twice Daily Thoracic Irradiation in Limited-Stage Small Cell Lung Cancer: An Overlap Weighted Analysis Michael Yan	15. Optimizing Site-Specific Diffusion Weighted Imaging in an MR-Linac Humza Nusrat
		12. Longitudinal In-Vivo Monitoring of Tissue Microvascular Heterogeneity in Irradiated Mice: Towards the Optimization of Stereotactic Body Radiotherapy Nader Allam	
2:45 PM	10 mins	Rapid Fire Presentations 3: Posters 17 – 23 (Moderated by Shane Harding)	Rapid Fire Presentations 4: Posters 24 – 30 (Moderated by Andrea McNiven)
2:55 PM	5 mins	<i>Closing Remarks</i> Michael Milosevic, UTDRO Vice Chair Research	
3:00 PM		<i>Pre-Recorded Video Poster Gallery</i>	

UTDRO RESEARCH DAY POSTERS

Details: May 5, 2021, 1:45 pm – 1:55 pm [Posters 1 – 16]

Location: Zoom

Rapid Fire Presentations 1: Posters 1 – 8 (Main Room)

Poster #	Abstract Title	Presenter
1	Optimal Management of Radiation Pneumonitis: Preliminary Findings of an International Delphi Consensus Study	Indu Voruganti
2	Development of Web-Based Quality-Assurance Tool for Radiotherapy Target Delineation for Head and Neck Cancer: Quality Evaluation of Nasopharyngeal Carcinoma	Jun Won Kim
3	4-Year PSA Response Rate as a Predictive Measure in Intermediate Risk Prostate Cancer Treated with Ablative Therapies: The SPRAT Analysis	Rachel Glicksman
4	A Prospective Study of MR-Guided Focal Salvage High Dose-Rate Brachytherapy for Radiorecurrent Prostate Cancer: Updated Results of 30 Patients	Mark Corkum
5	Therapeutic Targeting of PPAR Signaling in Cancer Treatment Related Lymphedema	Jennifer Kwan
6	Clinical Behavior and Outcome of HPV-positive Nasopharyngeal Carcinoma	JC Kenneth Jacinto
7	Retrospective Investigation of a Prostate SBRT Planning Strategy Utilizing Dynamic Planning	Hedi Mohseni
8	Your Voice Matters During COVID-19: Evaluation of Digital Divides Across a Tertiary Cancer Centre	Amir Safavi

Rapid Fire Presentations 2: Posters 9 – 16 (Breakout Room)

Poster #	Abstract Title	Presenter
9	Surgical Resection(s) Plus Stereotactic Radiosurgery (SRS) Versus SRS Alone for Large Brain Metastases: A Comparative Study	Enrique Gutierrez
10	An Articulated Robot for In-bore Sequential Needle Insertion under MRI-Guidance	Amanda Aleong
11	ATM Inhibitor AZD1390 Radiosensitization as a Strategy to Enhance Innate Immune Activation in Small Cell Lung Cancer (SCLC) Cell Lines and Syngeneic Genetically-Engineered Mouse Models (GEMM)	Xiaozhuo Ran
12	Excessive Transcription-Replication Conflicts are a Vulnerability of BRCA1-Mutant Cancers	Parasvi Patel
13	Dose Accumulation Comparison Between Adapt-to-Shape and Adapt-to-Position for MRL Adaptive SBRT Prostate Treatments at the Princess Margaret Cancer Centre	Christopher Johnstone
14	A Cross-Voxel Exchange Model for The Estimation of Kinetics Parameters of Tumour Tissue	Noha Sinno
15	Physician and Patient Reported Morbidity after MR-Guided Salvage Brachytherapy for Prostate Cancer	Inmaculada Navarro
16	Validation of the Truebeam Electron Monte Carlo Model Under Heterogeneous Tissue Conditions	Reza Askari

UTDRO RESEARCH DAY POSTERS [CON'T]

Details: May 5, 2021, 2:45 pm – 2:55 pm [Posters 17 – 30]

Location: Zoom

Rapid Fire Presentations 3: Posters 17 – 23 (Main Room)

Poster #	Abstract Title	Presenter
17	Patient-derived Xenograft Engraftment Predicts Oral Cavity Cancer Outcomes	Badr Id Said
18	Re-Evaluating Surgery and Re-Irradiation for Locally Recurrent Pediatric Ependymoma – A Multi-Institutional Study	David Mak
19	Impact of the COVID-19 Pandemic on Radiotherapy Patterns of Practice for Curative Intent Breast Cancer Patients	Donna Liao
20	Association of Tumour Volume and Outcomes in T3 Larynx Cancer with Organ Preservation Approach	Nauman Malik
21	Feedback Delivery in an Academic Cancer Centre: Reflections from an R2C2-Based Microlearning Course	Amir Safavi
22	Prostate SBRT on the MR-Linac at Odette Cancer Centre: Is the Longer Time Required in MRI-Guided Online Adaptation Prostate SBRT Justified?	Eyesha Hashim-Younus
23	Dosimetric Predictors of Toxicity and Quality of Life Following Single Fraction High Dose-Rate Prostate Brachytherapy	Mark Corkum

Rapid Fire Presentations 4: Posters 24 – 30 (Breakout Room)

Poster #	Abstract Title	Presenter
24	Limited-Stage Small Cell Lung Cancer: Outcomes Associated with Prophylactic Cranial Irradiation Over a 20-year Period at the Princess Margaret Cancer Centre	Tzen Szen Toh
25	Understanding the Potential Improvements in Neurocognition after Radiation Treatment of Brain Tumours with Proton Therapy	Mariana Petruccelli
26	Quantification of Radiation-Induced Microvascular Changes Using Optical Coherence Tomography and Dynamic Contrast Enhanced MRI	Jeffrey Zabel
27	The Contribution of Inflammasomes in RT-Induced Cell Fate and Anti-Tumour Immunity	Cindy Ha
28	Change in ADC as an Indicator of Radionecrosis	Matt Gwilliam
29	Strategic Training in Transdisciplinary Radiation Science for the 21st Century (STARS21): 5-year Prospective Evaluation of an Innovative Curriculum in Radiation Research	Parasvi Patel
30	Dynamic Contrast-Enhanced CT and MRI to Evaluate Response in Neuroendocrine Liver Metastases Treated with Everolimus and Radiation	John Hudson

UTDRO RESEARCH DAY ABSTRACTS – ORAL PRESENTATIONS

Oral Presentations: Section 1

01

A Machine Learning Challenge for Prognostic Modelling in Head and Neck Cancer Using Multi-modal Data

Michal Kazmierski, Mattea Welch, Sejin Kim, Chris McIntosh, Katrina Rey-McIntyre, Shao Hui Huang, Tirth Patel, Tony Tadic, Michael Milosevic, Fei-Fei Liu, Andrew Hope, Scott Bratman, and Benjamin Haibe-Kains

PURPOSE

Accurate prognosis for an individual patient is a key component of precision oncology. Radiomics aims to extract quantitative predictive and prognostic biomarkers from routine medical imaging, but evidence for computed tomography radiomics for prognosis remains inconclusive. We have conducted a machine learning challenge to develop an accurate model for overall survival prediction in head and neck cancer using clinical data extracted from electronic medical records (EMR) and pre-treatment radiological images, as well as to evaluate the true added benefit of radiomics for head and neck cancer prognosis.

METHOD

Using a large, retrospective cohort of 2552 patients, we assessed prognostic performance of 12 different approaches developed by several research groups at University Health Network, making use of engineered radiomics, deep learning on images, EMR information and combinations of those. To allow for unbiased comparison between different approaches, all participants had access to a public training dataset of 1802 patients, while 750 were held out for evaluation.

RESULTS

The best challenge submission used a deep multi-task logistic regression approach with 1 hidden layer on EMR data and tumour volume, achieving AUROC for 2-year survival prediction of .823 outperforming the best EMR-only model (AUROC = .798, $p < .05$), best radiomics-only model (AUROC = .766, $p < .05$), as well as the best model combining deep learning on images with EMR features (AUROC = .786, $p < .05$). We also used a 'wisdom of the crowds' ensemble approach to combine the predictions of all challenge submissions. The ensemble achieved slightly stronger performance than any individual model (AUROC=0.825), indicating that there might be complementary information between the different data modalities.

CONCLUSION

The challenge framework allowed us to evaluate a diverse collection of prognostic models in a large multi-modal dataset, demonstrating the value of machine learning in HNC prognostication, as well as the advantages of simple imaging features over several hand-engineered and deep radiomics approaches. Furthermore, our ensemble approach achieves excellent performance for both 2-year and lifetime risk prediction, establishing new state-of-the-art in HNC prognostic modelling.

02

Local control in Tumor-targeted Dose Escalation for Localized Prostate Cancer: A Report on the Target Study

Jerusha Padayachee, Noelia Sanmamed, Jenny Lee, Zihui Liu, Alejandro Berlin, Tim Craig, Bernadeth Lao, Alexandra Rink, Andrew Bayley, Charles Catton, Aravindhan Sundaramurthy, Warren Foltz, Andrew McPartlin, Sangeet Ghai, Eshetu Atenafu, Mary Gospodarowicz, Padraig Warde, Joelle Helou, Srinivas Raman, Cynthia Ménard, Peter Chung

PURPOSE

Tumor-targeted dose escalation may improve local control rates in patients with prostate cancer, leading to improved biochemical failure-free survival (bFFS). We report outcomes of dose escalation using a strategy of simultaneous integrated boost or HDR brachytherapy boost.

METHOD

Eighty patients with localized prostate cancer with gross tumor volume (GTV) identified on multiparametric magnetic resonance imaging (mpMRI) were enrolled in this phase 2 non-randomized trial (2012-2016). Patients with GTV \geq 5mm and less than 33% of total prostate volume were eligible. All patients received whole gland prostate volumetric arc therapy (VMAT), 76 Gy in 38 fractions. GTV dose escalation was delivered by integrated boost VMAT (IB-VMAT) of 95 Gy in 38 fractions (n=40); or MRI-guided HDR boost of 10 Gy in 1 fraction (n=40). Choice of dose escalation strategy was by physician and/or patient choice. The primary end-point was 3-year local control rates determined by MRI-guided biopsy and/or MRI alone. Toxicity data was collected using CTCAE v.4.0. Risk group categorization was comparable between the arms; 5% low-, 75% intermediate-, and 20% high-risk. Three patients received 6-months of concurrent/adjuvant ADT.

RESULTS

Median (IQR) follow-up was 55.2 months (48.1-71.4). The overall 5-year bFFS was 92% (95% CI, 85-99), with 5 patients developing biochemical relapse (BCR); 1 IB-VMAT, 4 HDR boost. Late G2 genitourinary (GU) toxicity was 22.5% and 27.5% in IB-VMAT and HDR boost, respectively. Late G2 gastrointestinal (GI) toxicity was 5% in each arm. Two G3 (1 GI, 1 GU) toxicities were seen in IB-VMAT. Local control data was available for 66 patients who agreed to the 3-year post-treatment biopsy (20) or MRI alone (46); 32 in IB-VMAT and 34 in HDR boost. Local control in the boost volume was achieved in 61 patients. One patient in the IB-VMAT arm had persistent disease on biopsy, and subsequently met criteria for BCR. At last follow-up of the 66 patients, 4 developed BCR with evidence of intraprostatic relapse outside the boost volume; 1 treated with IB-VMAT and 3 with HDR boost. These relapses appeared to correlate to sites of known microscopic disease at original diagnosis.

CONCLUSION

Dose escalation to mpMRI-defined GTV provided high rates of local and biochemical control with limited severe late toxicity. The majority of local treatment failures developed beyond the tumor-targeted volume, suggesting that other treatment intensification strategies may be required to further improve outcomes.

03

A Prognostic Model for Patients with Oligometastatic Disease Treated with Stereotactic Body Radiation Therapy

Hanbo Chen, Eshetu G. Atenafu, Darby Ertler, Ian Poon, Roi Dagan, Kristin J. Redmond, Matthew Foote, Serena Badellino, Tithi Biswas, Umberto Ricardi, Young Lee, Arjun Sahgal, Alexander V. Louie

PURPOSE

Stereotactic body radiation therapy (SBRT) is an increasingly important modality in the management of patients with oligometastatic disease (OMD). Though prospective clinical trials have demonstrated the benefits of SBRT in a variety of oligometastatic settings, there is currently limited data to guide patient selection and provide long-term prognostic information for OMD patients. The purpose of this study was to create a clinical prognostic model for overall survival (OS) for OMD patients treated with SBRT.

METHOD

A large, retrospective multi-institutional database of OMD patients treated with SBRT provided the data for model construction. Recursive partitioning analysis (RPA) was used to generate a prognostic model for OS that could account for complex interactions between baseline patient characteristics. The model was generated using a training set (75% of all samples) and internally validated using the reserved testing set. Model performance in the training and test sets were evaluated using log-rank tests, Harrell's C-statistic and time-dependent area under the receiver operating characteristics curve (AUC). All analyses were carried out in R.

RESULTS

A total of 1,033 patients were included in the analysis. RPA for OS revealed three risk groups. The low-risk group consisted of younger (<55) patients with favourable primary sites (hormone receptor/Her2-positive breast cancer, colorectal cancer or renal cell carcinoma) as well as any patient with a prostate cancer primary; the high-risk group consisted of patients with any other primary site who presented with non-pulmonary OMD within 24 months of the diagnosis of the primary disease; and the intermediate-risk group consisted of all other patients. The 5-year OS was 77.5 % (95% confidence interval: 63.1-91.9%), 32.3% (25.1-39.5%) and 12.1% (2.9-21.4%), respectively, for the low, intermediate and high-risk groups. Log-rank tests for difference in survival between the risk groups in both the training and test sets were highly significant ($p < 0.0001$). The model possessed good discriminative power with a C-statistic of 0.68 and time-dependent AUC of 0.72 in the training set, and there was an expected small reduction in these statistics in the test set (C-statistic: 0.65, AUC: 0.67).

CONCLUSION

An internally validated prognostic model for OS with good ability to distinguish between low, intermediate and high-risk OMD patients was generated. Subsequent external validation will be undertaken to demonstrate the robustness of this model to new data.

04

Hearing Loss After Radiation and Chemotherapy for Central Nervous System and Head and Neck Tumors in Children

Dana Keilty, Mohammad Khandwala, Zihui Amy Liu, Vicky Papaioannou, Eric Bouffet, David Hodgson, Ryan Yee, Normand Laperriere, Sameera Ahmed, Donald Mabbott, Sharon L. Cushing, Vijay Ramaswamy, Uri Tabori, Annie Huang, Ute Bartels, Derek S. Tsang

PURPOSE

Hearing loss (HL) is a serious secondary effect of treatment for head and neck (H&N) and central nervous system (CNS) tumors in children. Radiation and platinum chemotherapy independently increase the risk of HL; however, combined modality treatment is routinely used and the effect of chemoradiation on HL risk is not well-studied. Using chemotherapy and cochlear radiation (RT) doses, we created a model that predicts for HL, including a nomogram that can be used in the clinical setting to calculate the risk of clinically-significant HL.

METHOD

In this single institution retrospective study, 171 patients with H&N or CNS tumors were treated with radiation, with or without chemotherapy and had longitudinal (≥ 2) audiological evaluation. SIOP-Boston (SIOP) and Chang grades were assigned to 2,420 hearing assessments of 342 ears; analyses using SIOP grades are presented here. For the nomogram, SIOP grade ≥ 3 was considered clinically-significant HL (requiring hearing aids). An Andersen-Gill model for recurrent events was used to obtain inverse intensity weights to account for factors explaining the number of assessments. Multivariable weighted ordinal logistic regression was fitted to evaluate the effect of clinicopathologic features on HL. Clustered robust standard errors were calculated to account for intra-patient correlation.

RESULTS

Patients underwent a median of 6 (range 2-23) assessments over a median of 3.1 years from diagnosis to last audiogram (range 0.1-15.2 years). Cisplatin was given to 63% of patients and 34% received carboplatin. The mean cochlear doses on the right and left were 36.8 Gy (standard deviation [SD] 16.5) and 37.0 Gy (SD 16.2), respectively. Multivariable regression revealed that mean cochlear dose (odds ratio [OR] 1.04 per Gy, 95% confidence interval [CI] 1.02-1.05, $p < 0.001$), time since RT (OR 1.2 per year, 95% CI 1.2-1.3, $p < 0.001$), cisplatin use (OR 5.33, 95% CI 2.9-9.9, $p < 0.001$), and carboplatin use (OR 2.3, 95% CI 1.27-4.17, $p = 0.006$) were associated with increasing SIOP grade of HL; age at RT, hydrocephalus, surgery, amifostine, and laterality were not correlated with HL. There was no synergistic effect of RT and cisplatin (interaction term, $p = 0.4$) or RT and carboplatin (interaction term, $p = 0.9$). Cumulative incidence of high-frequency HL (> 4 kHz) was $> 50\%$ at 5 years post RT in those who received mean dose > 20 Gy to the cochlea, while incidence of HL across all frequencies continued to increase beyond 5 years post RT.

CONCLUSION

RT and chemotherapy have an additive, not synergistic, effect on HL risk. Mean cochlear radiation dose, time since radiation, and platinum chemotherapy use were associated with HL. This modelling can guide survivorship care by multidisciplinary pediatric oncology teams with respect to audiology follow-up in an effort to that ensure suitable educational accommodations and assistive devices are in place.

05

CNN-based Segmentation of Multiple Needles for Magnetic Resonance-guided Interventions

Amanda Aleong, Alejandro Berlin, Robert Weersink

PURPOSE

MRI offers the gold standard for delineating cancerous lesions in soft tissue. Needle-based interventions require the accurate placement of multiple long, flexible needles at the target site. The manual segmentation of needles in MR images to assess targeting accuracy is a challenging and time-consuming task. There is a need for automated needle segmentation to improve the efficiency and safety of MR-guided procedures. In this work, a 3D U-Net was trained to retrospectively segment needles in scans acquired during clinical MR-guided HDR prostate brachytherapy cases. The network successfully identified 95% of needles in the test set at a rate of 0.89 s/volume.

METHOD

Data was obtained from 35 patients who underwent HDR prostate brachytherapy (4280 images i.e. 214 image volumes). Multislice axial TSE verification scans (TE = 12 ms; TR = 2240 ms; resolution = 0.78x0.78 mm; slice thickness= 3 mm; matrix=256x256, no. of slices=20-30) were used to train and test a convolutional neural network with a U-Net architecture (depth = 4), built using Keras with a Tensorflow backend in Python3 2. A sequential model was used with an Adam optimizer and negative Dice coefficient loss function. A SeLU activation function was applied to each convolution layer and was followed by a dropout layer with a rate of 0.1. The network was trained on data from 30 patients (185 image volumes) for 100 epochs with a batch size of 4 image volumes and a validation split of

0.2. The remaining 5 patients (39 volumes) were used to test the performance of the model.

RESULTS

The network detected 749/757 (99%) of needles in the training set and 139/146 (95%) of needles in the test set with a prediction time of 0.89 s/image volume (Fig.1). The maximum Hausdorff Distance observed was 1.9 mm in-plane for the training and test sets. Both the axial and sagittal Hausdorff Distances observed are in agreement with the results obtained by Mehrtash et al. for single needle segmentation. Specifically, Mehrtash et al. reported that in 96% of the segmented cases the needle tip identified by the model was within 3 slices of the true tip location. This corresponds to the max sagittal Hausdorff Distance observed in this study in which all test cases were within 3 pixels provided that the needle was identified.

CONCLUSION

The results support the use of a U-Net model for the segmentation of multiple needles in MR image volumes. This strategy may be further adapted to MR images acquired in near real-time to facilitate the integration of real-time MR imaging in image-guided interventions. The rapid identification of needles in MR images will assist with the assessment of needle deflection during insertion and provide feedback for needle steering using robotic strategies.

06

Dosimetric Comparison in Malignant Glioma Patients Clinically Treated on Hybrid Magnetic Resonance Imaging (MRI)-Linac (MRL) versus Conventional Linac

Michael H. Wang, Anthony Kim, Mark Ruschin, Hendrick Tan, Hany Soliman, Sten Myrehaug, Jay Detsky, Zain Husain, Eshetu G. Atenafu, Brian Keller, Arjun Sahgal, Chia-Lin Tseng

PURPOSE

The Magnetic Resonance Imaging (MRI)-Linac (MRL) is a hybrid machine integrating a high field strength 1.5T MRI with a linear accelerator, providing superior soft tissue visualization of tumors and organs-at-risk (OARs) during treatment delivery. A special consideration for MRL radiotherapy is accounting for interactions of secondary electrons generated within the magnetic field, which can alter dose deposition at air-tissue interfaces. We evaluated dosimetric outcomes in clinically treated malignant glioma patients who received at least one fraction of radiotherapy on both the MRL and a conventional Linac.

METHOD

Thirty-seven glioma patients treated on both the MRL and a conventional Linac for adjuvant chemoradiotherapy between July 2019 and February 2021 were analyzed. Planning was completed on treatment planning systems (TPS) using a Monte-Carlo algorithm that accounts for magnetic field effects (Monaco v5.40) for the MRL, and a convolution-superposition algorithm (Pinnacle v9.8) for the conventional Linac. Dosimetric parameters of interest from the target, OARs, and air-tissue interface volumes for each patients' clinical treatment plans were extracted and compared. For 10 representative patients, in vivo skin doses during a single fraction of MRL and conventional Linac treatment were obtained using an Optically Stimulated Luminescent Dosimeter (OSLD) placed in a defined location on the patient's skin near the Planning Target Volume (PTV). Student's t-test and Wilcoxon signed-rank test were used to compare

parameters between Monaco and Pinnacle. Spearman's correlation was used to assess the relationship between in vivo OSLD measurements and TPS skin dose. Threshold for statistical significance was $p < 0.05$.

RESULTS

Most patients were treated for high grade glioma (76% Grade III or IV, 24% Grade II), and median PTV was 257.4 cm³ (range, 37.1-570.3 cm³). MRL and conventional Linac had similar V100, V95, D98, and D95 for PTV, and D3cc for optic chiasm, optic nerves, and each cochlea ($p = \text{NS}$). However, clinically delivered Monaco plans had significantly greater doses within air cavities (mean Dmean higher by 1.3 Gy, $p < 0.0001$) and skin (mean Dmean higher by 1.9 Gy, $p < 0.0001$; mean D2cc higher by 8.1 Gy, $p < 0.0001$; mean V20Gy higher by 7.2 cm³, $p < 0.0001$), compared to clinically delivered Pinnacle plans. In vivo OSLD skin readings were 14.5% greater for treatments delivered on the MRL ($p = 0.0027$), and were more accurately predicted by Monaco ($r = 0.95$, $p < 0.0001$) vs. Pinnacle ($r = 0.80$, $p = 0.0096$).

CONCLUSION

In this prospective study of clinically treated glioma patients on both MRL and conventional Linac, the dosimetric impact of the magnetic field was minimal for the target and standard OARs. However, higher doses to skin and air cavities were observed. In vivo correlation of dose to skin was more accurately predicted with Monaco. Future MRL planning processes are being designed to account for skin dosimetry and treatment delivery.

07

Access to Radiotherapy in Ghana: A Geospatial Analysis

Aba Scott, Alfredo Polo, Eduardo Zubizarreta, Charles Akoto-Aidoo, Michael Milosevic, Danielle Rodin

PURPOSE

Radiotherapy (RT) is a crucial component of comprehensive cancer care, but there are large global gaps in access. Within Ghana, a West African country with a population of 31 million people, there are only 3 RT centres with 5 external-beam (EBRT) and 2 high-dose rate (HDR) brachytherapy (BT) machines located in 2 cities in the south. This study aims to describe the gaps in RT capacity and geographic accessibility.

METHOD

A retrospective review of data from all RT centres in Ghana was done to determine the number of RT courses, EBRT fractions, and BT insertions delivered annually between 2018-2020. The additional RT capacity required for optimal utilization was estimated from GLOBOCAN 2020 cancer registry data and the Collaboration for Cancer Outcomes Research and Evaluation radiotherapy utilization rate (RUR) model for all cancers. Geospatial modeling was used to calculate the distances that patients currently need to travel to access RT, and how access would be improved with new RT centres strategically located throughout the country.

RESULTS

In 2020, Ghana delivered 1,794 RT courses and 34,624 EBRT fractions for all cancers, and performed 497 HDR BT insertions for cervical cancer (the 2nd

most common cancer in the country). Based on a RUR of 48%, an additional 9,730 RT courses, 188,948 EBRT fractions and 4,538 HDR BT insertions are required. This translates to 5 additional RT centers, each with 4 EBRT units and 1 HDR BT afterloader.

Based on the current capacity and distribution of RT centres, patients have a median one-way travel distance from their regional capital to the nearest RT centre of 157 km, with 54% of patients traveling less than 100 km, 15% traveling 100-150 km, 9% traveling 150-200 km, and 22% traveling more than 200 km. The North East, Upper East, and Upper West regions have the longest travel distances of 424 km, 533 km, and 439 km, respectively. Establishing a third RT centre in Tamale in northern Ghana would decrease median one-way travel distance from their regional capital to the nearest RT to 145.5 km, and the proportion of the population with a travel distance of over 200 km to 4%. Optimization of the location of other new centres is needed to further reduce the travel distances.

CONCLUSION

Ghana has a major national deficit of RT capacity, with significant geographic disparities among regions. Well-planned infrastructure scale-up that accounts for the population distribution can improve RT accessibility.

08

T-DM1 Increases the Risk of SRS-induced Radiation Necrosis in Her2+ Breast Cancer

Badr Id Said, Hanbo Chen, Katarzyna J. Jerzak, Sten Myrehaug, Chia-Lin Tseng, Jay Detsky, Zain Husain, Arjun Sahgal, Hany Soliman

PURPOSE

Stereotactic radiosurgery (SRS) is an important treatment modality in the management of breast cancer-related brain metastases (BrM). Recent research has found Trastuzumab emtansine (T-DM1) to be effective against Her2+ BrM. However, the risk of radionecrosis (RN) with T-DM1 in combination with SRS is unclear. The objective of this study was to investigate factors associated with RN post-SRS in patients with Her2+ BrM.

METHOD

Patients with Her2+ BrM treated with SRS at the Sunnybrook Odette Cancer Centre between 2010 and 2020 were retrospectively identified. The incidence of RN was determined on a lesion-by-lesion basis using serial brain imaging with or without histological confirmation. Clinical factors associated with RN, such as age, RT dose, lesion volume, intracranial location, total number of BrM, along with history of whole brain RT, and T-DM1 treatment were investigated with univariable and multivariable competing risks regression (MVR) using death from any cause as a competing risk factor. A p-value of <0.05 in MVR following backward selection was considered statistically significant.

RESULTS

67 patients with Her2+ BrM (223 lesions) treated with SRS were identified; among them, 21 (31.3%) were treated with T-DM1 post-SRS, including 14 (20.9%) who received T-DM1 within 12 months of SRS. The median follow-up was 15.6 (IQR 5.4-35.3) months. The 1-year, and 2-year risk of RN post-SRS was 6.7% (95% CI 2.7-10.7%), and 15.2% (95% CI 9.2-21.3%), respectively. MVR identified T-DM1 treatment post-SRS (HR 2.5, 95% CI 1.2-5.3, $p=0.02$) and RT dose with a biologically effective dose (BED) > 50.4 Gy (HR 2.4, 95% CI 1.1-5.1, $p=0.02$) as independent risk factors of RN. Patients treated with T-DM1 and SRS had a 25.2% (95% CI 12.8-37.6%) risk of RN at both 1- and 2-years post-T-DM1. The median time to RN after T-DM1 among the affected was 4.8 (95% CI: 3.8-25.6) months with 80% of all RN cases occurring within 12 months of T-DM1 treatment.

CONCLUSION

This study demonstrates that T-DM1 exposure post-SRS was independently associated with a higher risk of RN in Her2+ BrM patients. The potential side effects of brain-penetrating agents post-SRS merits greater awareness.

09

Hypofractionated Radiotherapy for Breast Cancer: Findings from an International ESTRO-GIRO Survey

Melinda Mushonga, Jessica Weiss, Amy Zhihui Liu, Bouchra Tawk, Osama Mohamad, Yolande Lievens, Danielle Rodin

PURPOSE

Hypofractionated radiotherapy (HR) for early breast cancer has been found to be equivalent to conventional fractionation (CF) in several large studies. More recently, accelerated HF regimens and HF in more advanced disease has been evaluated and adopted. Using data from the European Society of Radiation Oncology's (ESTRO) Global Impact of Radiotherapy in Oncology (GIRO) initiative survey on HF, this study aims to identify patterns, facilitators and barriers to uptake of breast cancer HF across World Bank income groups.

METHOD

The ESTRO-GIRO initiative administered an anonymous, electronic survey to radiation oncologists from January 2018 to January 2019. Details on physician demographics, clinical practice, preferred HF regimen for specific breast cancer clinical scenarios (curative and palliative), justifications and barriers for HF practices were collected. Curative scenarios included: node-negative (N0) following breast-conserving surgery (BCS) and mastectomy, and node-positive (N+) following BCS and mastectomy. The palliative scenario evaluated HF for symptom control. Factors associated with HF were assessed using multivariate logistic regression models.

RESULTS

A total of 1,434 physicians responded to the breast survey scenarios, with 1251 (87%) from high-income (HICs) and upper middle-income countries (UMICs) and

183 (13%) from low and low middle-income countries (LMICs). The most common HF fraction size, reported by 30% of respondents, was between 2.5 and 2.9 Gy delivered in a total of 15 fractions for curative indications (2.1-4Gy); only 1% of respondents reported using a 5-fraction regimen. For palliative indications, the most common HF fraction size, used by 23% of respondents, was between 3Gy and 3.5Gy in 10 fractions (2.1-6Gy). In N0 disease following BCS, there was no significant difference in use of hypofractionation in LMICs compared to HICs and UMICs. Respondents in Africa were less likely to hypofractionate compared to Europe (OR = 0.29, CI 0.12,0.69; p=0.006) and those using Cobalt-60 were less likely to hypofractionate than those with linear accelerators (OR = 0.55, CI 0.37,0.84; p=0.005). In the other curative scenarios, those in LMICs were more than twice as likely to hypofractionate compared to those in HICs and UMICs. There were no differences in use of HF across income groups for palliative symptom control. Published evidence was the most cited justification for HF (89%) across income groups. Lack of advanced technology was cited as a barrier by 14% in LMICs, compared to 5% in HICs and UMICs.

CONCLUSION

Apart from N0 disease following BCS, patterns of HF for breast cancer varied across income groups for curative indications, with minimal uptake of accelerated regimens. Targeted interventions are needed to address barriers to HF and support evidence-based utilization.

10

Province-Wide Analysis of Patient Reported Outcomes for Stage IV Non-Small Cell Lung Cancer

Michael C. Tjong, Mark Doherty, Hendrick Tan, Wing C. Chan, Haoyu Zhao, Julie Hallet, Gail Darling, Biniam Kidane, Frances C. Wright, Alyson Mahar, Laura E. Davis, Victoria Delibasic, Ambika Parmar, Nicole Mittmann, Natalie G. Coburn, Alexander V. Louie

PURPOSE

Stage IV NSCLC patients have significant disease and treatment-related morbidity. In Ontario, Canada, cancer patients complete Edmonton Symptom Assessment System (ESAS) questionnaires, a tool that elicits patients' self-reported severity of common cancer-associated symptoms at clinical encounters. ESAS domains are: anxiety, depression, drowsiness, appetite, nausea, pain, shortness of breath, tiredness and well-being. The purpose of this study is to examine moderate-to-severe symptom burden in the 12 months following a diagnosis of stage IV NSCLC.

METHOD

Using administrative databases and unique encoded identifiers, stage IV NSCLC diagnosed between January 2007 and September 2018 were evaluated for symptom screening with ESAS in the 12 months following diagnosis. Proportion of patients reporting moderate-to-severe score (i.e. ESAS ≥ 4) in each domain within 12 months were calculated. Patients reporting moderate-to-severe within the different ESAS domains of were plotted over time. Multivariable (MV) Poisson regression models with potential covariates such as age, sex, Elixhauser comorbidity index, income quintiles, and lung cancer treatments received were constructed to identify factors associated with moderate-to-severe symptoms.

RESULTS

Of 22,799 stage IV NSCLC patients, 13,289 (58.3%) had completed ESAS (84,373 unique assessments) in the year following diagnosis. Patients with older age, high comorbidity, and not receiving active cancer therapy were less likely to complete ESAS.

Most (94.4%) reported at least 1 moderate-to-severe score. Most prevalent moderate-to-severe ESAS symptoms within 12 months after diagnosis were tiredness (84.1%), lack of wellbeing (80.7%), low appetite (71.7%), and shortness of breath (67.8%); nausea was the least prevalent (34.6%). Most symptoms peaked at diagnosis and persisted in the year after diagnosis.

On adjusted MV analyses, patients with high comorbidity, low income, and urban residency were associated with increased moderate-to-severe symptoms. Moderate-to-severe scores in all ESAS symptoms were associated with delivery of radiotherapy within 2 weeks prior, while moderate-to-severe nausea, drowsiness, tiredness, low appetite, and lack of wellbeing were associated with delivery of systemic therapy within preceding 2 weeks.

CONCLUSION

In this population-based analysis of stage IV NSCLC PROs in the year following diagnosis, moderate-to-severe symptoms were highly prevalent and persistently high, underscoring the need to address supportive requirements in this at-risk population.

11

A Comparison of Hypofractionated and Twice Daily Thoracic Irradiation in Limited-Stage Small Cell Lung Cancer: An Overlap Weighted Analysis

Michael Yan, Samantha Sigurdson, Noah Greifer, Thomas Kennedy, Tzen Toh, Patricia Lindsay, Jessica Weiss, Katrina Hueniken, Christy Yeung, Vijithan Sugumar, Alexander Sun, Andrea Bezjak, John Cho, Srinivas Raman, Andrew Hope, Meredith Giuliani, Elizabeth Stuart, Timothy Owen, Alison Ashworth, Andrew Robinson, Fabio Ynoe de Moraes, Geoffrey Liu, Benjamin Lok

PURPOSE

Despite evidence for the superiority of twice daily (BID) radiotherapy schedules, their utilization in practice remains logistically challenging. Hypofractionation (HFRT) is a commonly implemented alternative. We aim to compare the outcomes and toxicities in limited stage small cell lung cancer (LS-SCLC) patients treated with hypofractionated versus BID schedules.

METHOD

A bi-institutional retrospective cohort review was conducted of LS-SCLC patients treated with BID (45Gy/30 fractions) or HFRT (40Gy/15 fractions) schedules from 2007-2019. Overlap weighting using propensity scores were performed to balance observed covariates between the two radiotherapy schedule groups. Effect estimates of radiotherapy schedule on overall survival (OS), locoregional recurrence (LRR) risk, thoracic response, any grade 3+ (including lung, and esophageal) toxicity were determined using multivariable regression modelling. E-values were used to assess the sensitivity of effect estimate to unobserved confounding.

RESULTS

A total of 173 patients were included in the overlap weighted analysis, with 110 patients having received BID treatment, and 63 treated by HFRT. The 5-year OS for the overlap weighted cohort was 24.3% (95% CI, 16.1-36.6), and specifically 22.1% (95% CI, 12.7-38.5) and 26.6% (95% CI, 14.4-49.0%) when stratified by BID and HFRT cohorts specifically. The 5-year LRR risk for the same cohorts after overlap weighting were 68.9% (95%CI, 59.2-80.1), 68.9% (95% CI, 56.6-83.8), and 69.2% (95% CI, 55.3-86.6), respectively. Multivariable regression modelling did not reveal any significant differences in OS (hazard ratio [HR] 1.67, $p = 0.38$), LRR risk (HR 1.48, $p = 0.38$), CRT response (odds ratio [OR] 0.23, $p = 0.21$), any grade 3+ toxicity (OR 1.67, $p = 0.33$), grade 3+ pneumonitis (OR 1.14, $p = 0.84$), or grade 3+ esophagitis (OR 1.41, $p = 0.62$). These effect estimates were consistent between unweighted and overlap weighted cohorts.

CONCLUSION

HFRT, in comparison to BID radiotherapy schedules, does not appear to result in significantly different survival, locoregional control, or toxicity outcomes.

12

Longitudinal In-vivo Monitoring of Tissue Microvascular Heterogeneity in Irradiated Mice: Towards the Optimization of Stereotactic Body Radiotherapy

Nader Allam, W. Jeffrey Zabel, Blake Jones, Valentin Demidov, Edward Taylor, and I. Alex Vitkin

PURPOSE

Pancreatic ductal adenocarcinoma (PDA) is projected to become the second most lethal cancer type by the year 2030. However, stereotactic body radiotherapy (SBRT) has demonstrated some improved tumour control compared to conventional treatments where surgical resection is not possible. SBRT's efficacy seems to involve its effects on the tumour microvasculature (diameter $\sim 10\text{-}30\mu\text{m}$). We therefore hypothesize that by monitoring the temporal changes in the morphology of the irradiated microvasculature, macroscopic tumour response to SBRT may be predicted. We have previously reported on the potential predictive power of the vascular volume density (VVD) metric for gross-tumour response to high single-dose irradiation in mice. Here we present the results on a metric more reflective of tissue vascular heterogeneity, the diffusion-limited fraction (DLF), defined as the proportion of tissue beyond a given distance from the nearest blood vessel; DLF may thus be radiobiologically important in determining SBRT's outcome.

METHOD

NOD-Rag1null IL2rgnull (NRG) mice ($n=21$) were subcutaneously inoculated dorsally with BxPC3-DsRed PDA patient-derived-xenograft cell-line. Once tumours reached a diameter of 3-4mm, dorsal-skinfold window-chambers were installed to enable longitudinal intravital optical monitoring in response to a range of high-single fraction irradiation (10-30Gy) over the course of 2 months prior- and post- irradiation. Gross-tumour response was assessed through caliper measurements and epi-fluorescence imaging for tumour viability quantification. Blood microangiography of the tumours was performed through speckle-variance (sv) processing of volumetric structural images acquired at $4\times 25\times 25\ \mu\text{m}^3$ (axial \times lateral 2) resolution up to $\sim 1\text{mm}$ in depth via swept-

source optical coherence tomography (OCT). DLF at a distance threshold of $150\mu\text{m}$ (DLF150) time course was computed from the binarized 3D microvascular maps through application of the 3D Euclidean transform via MATLAB. Histological corroboration of in-vivo DLF measurements was performed by defining an area-based DLF metric (DLAF). DLAF was computed from CD31 vessel-staining on multiple sections across the tumour to account for tissue microvascular heterogeneity and compared to multiple OCT cross-sections.

RESULTS

Maximum DLF150 attained was proportional to total delivered dose, consistent with known early-responding tissue response kinetics. DLF150 in unirradiated controls exhibited a small gradual decrease, likely indicative of uninterrupted tumour development. Change in DLF150 was also observed to precede macroscopic tumour response, however no conclusions regarding causality can yet be made. Trends in histological DLAF and in DLF derived from svOCT were mutually consistent.

CONCLUSION

A new vascular biomarker with potential predictive power for longitudinally monitoring the effectiveness of accelerated hypofractionated radiotherapy, such as SBRT, is presented. DLF reports on avascular volume fractions and may thus contain important functional information pertaining to chronic hypoxia, a major indicator of poor tumour prognosis. Investigations currently underway seek to correlate this (and other morphological metrics acquired via OCT) to magnetic resonance angiography, to enhance clinical translatability of developed predictive microvascular metrics models towards adaptive radiotherapy.

13

Quantitative Texture Analysis of Optical Coherence Tomography Images for Early Detection of Tumour Response to Radiotherapy

Valentin Demidov, Natalia Demidova, Layla Pires, Olga Demidova, Costel Flueraru, Brian C. Wilson, Alex Vitkin

PURPOSE

To develop a microscopic resolution technique based on optical coherence tomography (OCT) for tumour delineation and early detection of its response to radiation therapy (RT).

METHOD

OCT, an effective label-free high-resolution 3D imaging technique with 1-3 mm penetration depth, was used for in-situ, noninvasive real-time investigation of tumour micromorphology for 5 weeks after 15Gy single dose RT in NRG mouse pancreatic cancer model. A novel scheme was implemented to irradiate only half of each tumour to a) observe the differential changes truly caused by radiation (as opposed to the dynamics of tumour evolution unrelated to RT) and b) reduce the number of experimental animals by having a non-treated “reference” from the same tumour. To detect early RT-induced changes, a fully automatic volumetric tumour delineation technique was developed, employing quantitative OCT image speckle analysis based on gamma distribution fits of image voxel intensity histograms. Accurate tumour boundary detection was confirmed using epi-fluorescence microscopy, combined photoacoustic-ultrasound imaging, and histology. The temporal evolution of the gamma distribution fit parameters following RT was studied to gain insights into the radiobiological response of irradiated tissues.

RESULTS

Computed parametric images substantially improved OCT contrast relative to regular structural images, enabling accurate 3D tumour delineation; this was especially true in settings involving tumours that were highly heterogeneous, were not well circumscribed (presenting a diffuse rather than a sharp border),

and were aggressively invading surrounding tissues. A total of eleven longitudinal observations of each BxPC-3 pancreatic tumour were recorded. Throughout the monitoring period, the treated part of each tumour gradually shrunk, while the untreated part progressively increased in size (over 5 weeks). OCT-derived microvasculature maps demonstrated gradual vascular destruction of the treated part of each tumour starting from week 1, followed by revascularization closer to week 5. In contrast, the untreated tumour exhibited continuous enlargement and growing complexity of vascular networks. The same Gamma distribution fit parameters (k , θ) used for tumour delineation also served as early biomarkers of tumour response to RT, as radiation likely caused characteristic microstructural transformations at the cellular level that are known to change the optical properties of tissues. Significant changes in the Gamma fit parameter values of the treated regions were detected and compared to the non-irradiated regions of each tumour that showed relatively steady behavior. The fitting parameter k was ~ 20 times less sensitive than fitting parameter θ to the 15Gy treatment: its maximum change was at max $\sim 25\%$ decrease from initial values, compared to a greater than 500% rise in θ after week 3.

CONCLUSION

The novel approach to assessment of tumour response to radiotherapy made use of high-resolution 3D optical images, demonstrating high accuracy and objective nature in the volumetric separation of tumour and normal tissues, and the sensitivity of the fitting parameters to radiation-induced tissue changes. Overall, the developed methodology enables hitherto impossible longitudinal studies for detecting subtle tissue alterations stemming from therapeutic RT insult.

14

Predictive Modeling for Rapid Online Evaluation of Plan Quality During Intraoperative Gynecological Brachytherapy

Priscilla Dreyer, Moti Paudel, Eric Leung, Amandeep Taggar, Matt Wronski

PURPOSE

The current standard of care for locally advanced gynecological cancers is external beam radiotherapy with brachytherapy boost to the high risk clinical target volume (HRCTV). Intraoperative treatment planning for brachytherapy boost is performed while the patient is under anesthesia, therefore an acceptable plan must be achieved within a limited timeframe. The purpose of this work is to develop a model that can predict the plan quality, thereby allowing the planning team to evaluate if an acceptable plan has been achieved, or if additional optimization is required.

METHOD

Using an internal database of patients treated with gynecological intraoperative brachytherapy between May 2016 and June 2020 at The Odette Cancer Center, two different models were developed using MATLAB (Mathworks, R2018b); (1) a distanced based model and (2) an iterative computational model. The distance model evaluates the achieved HRCTV D90/OAR D2cc as a function of quality metric OAR distance to HRCTV. The iterative model evaluates the achieved HRCTV D90/OAR D2cc as a function of the quality metric predicted HRCTV D90/OAR D2cc. Both models employ a point cloud representation of the HRCTV and the organs at risk (OAR). The iterative model further accounts for implant quality which is represented by the activated dwell positions. Regression analysis was performed on both

models to evaluate the ability of each quality metric in predicting the achieved HRCTV D90/OAR D2cc in the accepted clinical treatment plan.

RESULTS

The distance based model is less precise in its ability to predict achieved HRCTV D90/OAR D2cc ($R^2=0.83$) in comparison to the iterative model ($R^2=0.97$) indicating that the quality of implant, which is accounted for in the iterative model, is necessary for accurate modeling of achieved HRCTV D90/OAR D2cc. Assuming an external beam dose of 45 Gy in 25 fractions, the iterative model can consistently predict the combined EQD2 dose from brachytherapy and external beam treatment to within $\pm 7\%$, with 95% confidence.

CONCLUSION

The iterative model can be used during brachytherapy treatment planning to rapidly determine whether a new intraoperative treatment plan is consistent with the plan quality that has been achieved previously within the center. Future work will include demonstrating the utility of this model in a clinical setting by evaluating how well it can distinguish between acceptable plans and plans requiring further optimization, for the given constraints of patient anatomy and implant quality.

15

Optimizing Site-Specific Diffusion Weighted Imaging in an MR-Linac

Humza Nusrat, Liam Lawrence, Rachel Chan, Angus Lau, Alyaa Elzibak, Brige Chugh, Arjun Sahgal, Brian Keller

PURPOSE

The Diffusion weighted imaging (DWI) is sensitive to changes in tumor microstructure and can be used to non-invasively monitor radiotherapy treatment response. Despite being clinically available in MR-scanners, DWI can be further optimized in MR-guided radiotherapy systems. Maximum b-value is an important sequence parameter that controls the amount of diffusion weighting; high diffusion weighting leads to noise and less accurate apparent diffusion coefficient (ADC) estimates. MR-Linac users follow the recommended maximum b-value of 500 s/mm², however, higher maximum b-values are routinely used for DWI in sites such as the brain. The goal of this work was to optimize DWI in an MR-Linac using a standardized phantom.

METHOD

DWI sequences for brain, prostate, and abdomen were optimized with respect to maximum b-value and number of signal averages (NEX). DWI scans of the NIST-QIBA phantom (High Precision Devices, Boulder, USA) were conducted in the Elekta Unity MRLinac's (Elekta AB, Stockholm, Sweden) Philips Marlin 1.5T MR scanner. ADCs were estimated by fitting with offline reconstruction (MATLAB). Maximum b-value and NEX were varied and differences between measured and manufacturer-specified ADC

were reported. The impact of varying NEX on scan duration was also quantified. models to evaluate the ability of each quality metric in predicting the achieved HRCTV D90/OAR D2cc in the accepted clinical treatment plan.

RESULTS

For the brain sequence, maximum b-value achieving accurate ADC was 3,000 s/mm² ($\pm 4.0\%$ of standard across all diffusion vials). For all three sites, fitting with a subset of b-values below 400 s/mm² reduced ADC accuracy ($\pm 17.6\%$, 22.3%, 24.1% for brain, prostate and abdomen, respectively). Reducing NEX from clinical protocol to the scanner's minimum resulted in underestimation of ADC by 14.3% ($\pm 1.7\%$), 18.4% ($\pm 5.1\%$), and 17.5% ($\pm 4.3\%$) for the brain, prostate, and abdomen sequences, respectively but reduced average scan duration from 5.8 to 1.1 minutes.

CONCLUSION

Site-specific DWI sequences were optimized for ADC accuracy with respect to maximum b-value and scan time using a standardized phantom. Future work involves repeating this methodology in vivo.

UTDRO RESEARCH DAY ABSTRACTS – POSTER PRESENTATIONS

Poster Presentations: Section 1

01 Optimal Management of Radiation Pneumonitis: Preliminary Findings of an International Delphi Consensus Study

Indu S. Voruganti, Cicely Cunningham, Lorraine McLeod, Stephen Harrow, Alexander V. Louie

PURPOSE

Radiation pneumonitis (RP) is a dose-limiting toxicity for lung cancer patients undergoing radiotherapy (RT) and systemic therapy. As the optimal practice for diagnosis, management and follow-up for RP is variable, we sought to establish expert consensus recommendations.

METHOD

International leaders in multidisciplinary thoracic oncology were invited to participate (n = 31) in this delphi consensus-building process. Following literature review on RP, open-ended questions related to knowledge, risk-reduction, diagnosis and treatment were generated for Round 1. Responses were used to generate 37 statements regarding RP diagnosis and management for Round 2. In this round, participants rated their agreement/disagreement with statements using a 5-point Likert scale, with oncologists receiving a survey with 2 additional items focused on planning technicalities. Consensus was achieved once $\geq 75\%$ of respondents agreed with a statement. A final round to establish consensus in unresolved areas is planned.

RESULTS

Round 1 had a 74% response rate (n=23; 12 radiation oncologists, 5 clinical oncologists, 6 respirologists), and Round 2, a 61% response rate (n=19; 15 oncologists, 4 respirologists). Of the 37 Round 2 statements, 36 received $\geq 75\%$ agreement. By the end of Round 2, there was consensus opinion with agreement on the following: (1) risk stratification and mitigation should include patient factors (exposures, ILD, autoimmune and genetic conditions, COPD, emphysema, previous RT, and demographics); (2) minimizing RP risk through treatment planning (tight PTV margins, limiting dose to normal lung, dose/fractionation, IV contrast, motion management, IMRT/VMAT, daily imaging, and meeting constraints for V20 and MLD) should be utilized when possible; (3) diagnosis should be based on symptoms, exam, temporal relationship to treatment, imaging, and common toxicity grading scales; (4) Treatment of RP should be multidisciplinary, with oncologists and respiratory physicians, and should involve administration of oral steroids with gastroprotection, starting with 60 mg PO prednisolone or equivalent, for a duration of 2 weeks, with a taper of 10 mg in the daily dose per week, or for severe pneumonitis, IV methylprednisolone for 3 days before PO. Treatment adjuncts may include oxygen, inhalers, and antibiotics; (5) in differentiating drug-related pneumonitis vs. RP, standard review of patients receiving immunotherapy, per ASCO/ESMO guidelines, is insufficient to identify early pneumonitis, and thus it would be helpful to develop guidelines which recognize the additive nature of toxicities.

CONCLUSION

Responses from international thoracic oncology experts highlight areas lacking consensus in the diagnosis and management of RP. These data will inform the development of final consensus statements to provide practical guidance on diagnosis and management of RP.

02 Development of Web-Based Quality-Assurance Tool for Radiotherapy Target Delineation for Head and Neck Cancer: Quality Evaluation of Nasopharyngeal Carcinoma

Jun Won Kim, Joseph Marsilla, Michal Kazmierski, Denis Tkachuk, Shao Hui Huang, Wei Xu, John Cho, Jolie Ringash, Scott Bratman, Benjamin Haibe-Kains, Andrew Hope

PURPOSE

We developed QUANNOTATE, a new web-application for rapid review of radiotherapy (RT) target volumes, and used it to evaluate the relationship between target delineation compliance with the international guidelines and treatment outcomes in nasopharyngeal carcinoma (NPC) patients undergoing definitive RT.

METHOD

The dataset used for this study consists of anonymized CT simulation scans, RT structures, and clinical data of 332 pathologically confirmed NPC patients treated with intensity-modulated RT between July 2005 and August 2017. We imported the contours of intermediate risk clinical target volumes of the primary tumor (IR-CTVp) receiving 56 Gy into QUANNOTATE. We determined inclusion of anatomic sites within IR-CTVp in accordance with 2018 International guideline for CTV delineation for NPC and correlated the results with time to local failure (TTLF) using Cox-regression.

RESULTS

At a median follow-up of 5.6 years, 5-year TTLF and overall survival rates were 93.1% and 85.9% respectively. The most frequently non-guideline compliant anatomic sites were sphenoid sinus (n = 69, 20.8%), followed by cavernous sinus (n = 38, 19.3%), left and right petrous apices (n = 37 and 32, 11.1% and 9.6%), clivus (n = 14, 4.2%), and right and left foramen rotundum (n = 14 and 12, 4.2% and 3.6%). Among 23 patients with a local failure (6.9%), the number of non-compliant cases were 8 for sphenoid sinus, 7 cavernous sinus, 4 left and 3 right petrous apices, and 2 clivus. Compared to conforming cases, cases which did not contour the cavernous sinus had a higher local failure (LF) rate (89.1% vs 93.6%, p= 0.013). Multivariable analysis confirmed that lack of cavernous sinus contouring was prognostic for LF.

CONCLUSION

QUANNOTATE allowed rapid review of target volumes in a large patient cohort. Despite an overall high compliance with the international guidelines, undercoverage of the cavernous sinus was correlated with LF.

03 4-year PSA response rate as a predictive measure in intermediate risk prostate cancer treated with ablative therapies: The SPRAT analysis

Rachel Glicksman, Amar U Kishan, Alan J Katz, Constantine A Mantz, Sean P Collins, Donald B Fuller, Michael L. Steinberg, David Shabsovich, Liying Zhang, Andrew Loblaw

PURPOSE

There is a lack of early predictive measures of outcome for patients with intermediate-risk prostate cancer (PCa) treated with stereotactic body radiotherapy (SBRT). We aim to explore 4-year PSA response rate (4yPSARR) as an early predictive measure.

METHOD

Individual patient data from 6 institutions for patients with intermediate-risk PCa treated with SBRT between 2006-2016 with a 4-year (42-54 months) PSA available were analyzed. Cumulative incidences of biochemical failure and metastasis were calculated using Nelson-Aalen estimates and overall survival was calculated using the Kaplan-Meier method. Biochemical failure-free survival was analyzed according to 4yPSARR with groups dichotomized based on PSA ≤ 0.4 ng/mL or > 0.4 ng/mL and compared using the log-rank test. Multivariable competing risk analysis was performed to predict for biochemical failure and development of metastasis.

RESULTS

Six-hundred thirty-seven patients were included, including 424 (67%) with favorable and 213 (33%) with unfavorable intermediate-risk disease. Median follow-up was 6.2 years (IQR 4.9-7.9). The cumulative incidence of biochemical failure and metastasis, and overall survival at 6 years was 7%,

0.6% and 97%, respectively. The cumulative incidence of biochemical failure at 6 years if 4yPSARR ≤ 0.4 ng/mL was 1.7%, compared to 27% if 4yPSARR > 0.4 ng/mL ($p < 0.0001$). On multivariable competing risk analysis, 4yPSARR was a statistically significant predictor of biochemical failure-free survival (sHR 15.3, 95% CI 7.5-31.3, $p < 0.001$) and metastasis-free survival (sHR 31.2, 95% CI 3.1-311.6, $p = 0.003$).

CONCLUSION

4yPSARR is an encouraging early predictor of outcome in patients with intermediate-risk PCa treated with SBRT. Validation in prospective trials is warranted.

04 A Prospective Study Of MR-Guided Focal Salvage High Dose-Rate Brachytherapy for Radiorecurrent Prostate Cancer: Updated Results of 30 Patients

Mark T. Corkum, Gerard Morton, Andrew Loblaw, Chia-Lin Tseng, Jure Murgic, Ananth Ravi, Melanie Davidson, Matt Wronski, Masoom Haider, Hans T. Chung

PURPOSE

Salvage therapies for localized radiorecurrent prostate cancer often carry significant short- and long-term morbidity. Focal salvage high dose rate (HDR) brachytherapy is an appealing treatment technique which delivers an ablative dose of radiotherapy to the portion of the prostate containing recurrent disease; however, limited prospective data is available. We sought to explore the toxicities, health related quality of life and efficacy of focal salvage HDR brachytherapy after previous definitive radiotherapy.

METHOD

Patients with locally recurrent prostate cancer after previous external beam radiotherapy (EBRT) and/or brachytherapy were enrolled on a prospective clinical trial. Patients received MRI-guided, ultrasound-based focal HDR brachytherapy delivered over two fractions of 13.5 Gy delivered 1-2 weeks apart. Adjuvant androgen deprivation therapy (ADT) was not used. Toxicity was measured using CTCAE v4. Posttreatment response was evaluated using MRI 1-2 years after salvage. Biochemical failure was defined as PSA nadir + 2ng/mL.

RESULTS

Thirty patients were treated between November 2012 and September 2019. Median follow-up was 35 months (range: 13 – 92 months). Fifteen patients

were initially treated with EBRT, 3 with low dose rate (LDR) brachytherapy monotherapy, 1 with EBRT and LDR brachytherapy boost, 2 with EBRT and HDR brachytherapy boost, and 9 with HDR brachytherapy as monotherapy (all 19 Gy in a single fraction). Median clinical target volume (CTV) at time of salvage was 5.22 mL (range: 2.18 – 15.71 mL), corresponding to a median of 20.0% of the prostate volume (range: 8.8% – 39.2%). Median PSA at salvage was 4.46 ng/mL (range: 0.99 – 11.63 ng/mL). The median CTV V100 was 96.5% (range: 90.5% – 99.5%), and median CTV D90 was 15.1 Gy per fraction (range: 13.6 – 18.1 Gy). Seventeen patients experienced subsequent biochemical failure, and 9 have received ADT and/or further local salvage. No patients have died from prostate cancer. Median time to biochemical failure was 41.5 months, and median time to ADT/salvage therapy was 70.6 months. The three-year biochemical failure-free event rate was 61.8% (95% CI 44.0 – 86.6%), and three-year ADT/salvage therapy-free event rate was 86.0% (95% CI 74.1 – 99.8%). No acute grade ≥ 3 GU/GI toxicity was observed. One late grade 3 GU toxicity event occurred, cystitis at 42 months post treatment, which did not persist on follow-up. No late grade ≥ 3 GI toxicity was seen. Of the 28 patients who had a post-treatment MRI, 26 had evidence of a local treatment response.

CONCLUSION

In our updated results, we found focal salvage HDR brachytherapy is well tolerated with a favourable side effect profile and 3-year biochemical control rates in line with other salvage therapies for radiorecurrent prostate cancer. While early MRI response at the treated site is common, this does not preclude subsequent biochemical failure.

05 Therapeutic Targeting of PPAR Signaling in Cancer Treatment Related Lymphedema

Jennifer Kwan, Pierre Antoine Bissey, Willa Shi, Justin Williams, Siba Haykal, Benjamin Haibe-Kains, Kenneth W. Yip, Fei-Fei Liu

PURPOSE

Lymphedema secondary to cancer treatment affects up to 1 in 5 cancer survivors. It is an irreversible late normal tissue toxicity characterized by swelling and scar formation (fibrosis) of the affected limb with physical and psychosocial health consequences for patients. Recent evidence reveals changes in peroxisome proliferator-activated receptor (PPAR) signaling as an underlying pathology of this disease. PPAR agonists have demonstrated therapeutic benefit in other fibrotic conditions; their role in lymphedema, however, remains unclear.

METHOD

In this study, RNA-sequencing of human and murine tissues with and without lymphedema was performed. Samples included: human lymphedema (n=4), human control (n=5, matched for demographics and cancer history), murine lymphedema (n=12), and murine control (n=9). Pathway enrichment analysis was performed. An in vitro model of lymphedema fibrosis using cultured transforming growth factor beta (TGFB)-stimulated fibroblasts and an in vivo model of lymphedema using a murine surgical model of tail lymphedema were utilized to evaluate the effects of PPAR agonists on gene expression and fibrotic protein expression (pro-collagen Ia1, collagen) in lymphedema compared to controls.

RESULTS

RNA-sequencing of tissue from human and murine lymphedema and control subjects identified that suppression of PPAR signaling was a hallmark of lymphedema fibrosis on pathway enrichment analysis (FDR<0.01). In the murine model, PPAR signaling gene expression changes co-occurred with fibrotic deposition beginning as early as two weeks after lymphedema development, and continued for at least 35 weeks. Treatment of TGFB-stimulated fibroblasts with a PPAR agonist resulted in an increase in expression of PPAR genes and suppression of COL1 α 1 gene expression (n \geq 9 per group, q<0.05) as well as reduction in the secretion of fibrotic proteins: pro-collagen Ia1 on ELISA (n \geq 8 per group, p<0.0001) and collagen I on Western blotting. PPAR agonist treatment of the murine model of lymphedema resulted in a significant reduction in lymphedema fibrosis as measured by trichrome collagen staining (n \geq 4 per group, p<0.05).

CONCLUSION

These data, for the first time, demonstrated the value of upregulating PPAR signaling to treat lymphedema. For this condition, which to date, has no cure, repurposing PPAR agonists for lymphedema treatment is a highly promising therapeutic opportunity, which warrants further investigation.

06 Clinical Behavior and Outcome of HPV-positive Nasopharyngeal Carcinoma

JC Kenneth Jacinto, Shao Hui Huang, Jie Su, John Kim, Brian O'Sullivan, Jolie Ringash, John Cho, Andrew Hope, Scott Bratman, Meredith Giuliani, Ali Hosni, Ezra Hahn, Anna Spreafico, Aaron Hansen, David Goldstein, Li Tong, Bayardo Perez-Ordonez, Ilan Weinreb, Wei Xu, John Waldron

PURPOSE

Nasopharyngeal cancer (NPC) is traditionally EBV related. However, HPV-positive (HPV+) NPC seems to be increasing in the Western world recently. We describe the clinical behavior and outcomes of HPV+NPC compared to EBV-positive (EBV+) NPC and HPV+ oropharyngeal cancer (OPC).

METHOD

All newly diagnosed non-metastatic viral-related NPC and OPC treated with IMRT from 2005-2020 were reviewed. Viral etiology was confirmed by p16 staining, supplemented by real-time polymerase chain reaction of DNA for high-risk HPV, and EBER in-situ hybridization for EBV. Clinical characteristics of HPV+ and EBV+NPC were compared using the 2005-2020 NPC cohort, while locoregional control (LRC), distant control (DC) and overall survival (OS) were compared using the 2005-2018 cohort to allow sufficient follow-up among HPV+NPC, EBV+NPC and HPV+OPC patients. Presenting signs/symptoms of HPV+NPC and EBV+NPC were compared by 1:1 matched pair analysis (matched to T category, N category, smoking, age, gender, WHO type IIA vs IIB, and diagnosed year). Multivariable analysis (MVA) evaluated the cohort effect adjusting for confounders.

RESULTS

A total of 29 HPV+NPC (25 Caucasians and 4 Asians), 422 EBV+NPC, and 1310 HPV+OPC were eligible. HPV genotype was available in 20/29 HPV+NPC patients: 14 (70%) HPV-16; 6 (30%) non-HPV-16. Compared to EBV+NPC overall, HPV+NPC patients were older (median age: 58 vs 52 years, $p=0.006$), were predominantly Caucasian (86% vs 15%, $p<0.001$), and had higher T (T2-4: 86% vs 68%, $p=0.039$) but similar N categories (N2-3: 66% vs 58%, $p=0.44$). Within the matched cohort, more HPV+NPC patients complained of local pain vs EBV+NPC (28% vs 3%, $p=0.025$) but a similar proportion had cranial neuropathy (21% vs 31%, $p=0.55$). No significant difference existed in gross tumor volume or involved lymph node distribution ($p>0.05$). Median follow-up for HPV+NPC, EBV+NPC and HPV+OPC was 3.1, 6.0, and 5.2 years respectively. Compared to EBV+NPC ($n=374$), HPV+NPC ($n=20$) had similar 3-year LRC (95% vs 90%, $p=0.416$) and OS (84% vs 89%, $p=0.137$), but non-significantly lower DC (75% vs 88%, $p=0.13$). Compared to HPV+OPC ($n=1310$), HPV+NPC also had similar 3-year LRC (95% vs 94%, $p=0.74$) and OS (84% vs 87%, $p=0.307$), but lower DC (75% vs 90%, $p=0.036$). The difference in DC became non-significant in MVA [HR 1.83 (0.73-4.58), $p=0.19$] after adjusting for T category, N category, smoking pack-years, and chemotherapy.

CONCLUSION

HPV+NPC is an emerging entity, of which about one-third are caused by non-HPV-16 genotype. Compared with the more common EBV+NPC cases, HPV+NPC presents with more local pain and advanced T categories but has similar outcomes. HPV+NPC also has similar outcomes to HPV+OPC except that DC is lower in univariable analysis, possibly attributable to higher T category and non-HPV-16 genotypes. There may be a role for modification of systemic therapy in HPV+NPC to address distant failure risk.

07 Retrospective Investigation of a Prostate SBRT Planning Strategy Utilizing Dynamic Planning

Hedi Mohseni, Agnes Cheung, Charles Cho, Jason Wong, Louis Fenkell, Beibei Zhang

PURPOSE

This study investigates the feasibility of a planning strategy for implementing prostate SBRT with decreased PTV margins without fiducials or rectal spacers, to achieve the same curative treatment intent while decreasing the number of fractions.

METHOD

For patients receiving standard curative radiotherapy (60 Gy in 20 fractions) who may qualify for SBRT (40 Gy in 5 fractions, PACE-B protocol), a standard plan and an SBRT plan will be generated. If the SBRT plan does not meet protocol the patient will be deemed ineligible for SBRT and will receive a standard fractionation. If the SBRT plan is acceptable, the patient will proceed with standard treatment for 4 fractions. The acceptable SBRT plan(s) will be copied onto each CBCT using Dynamic Planning in Pinnacle Treatment Planning System with all IGRT shifts applied, and dose will be reconstructed using bulk density override. CTV will be rigidly propagated and reviewed/modified as necessary. If reconstructed CTV coverage was sufficient for these fractions, it is hypothesized that the proposed margin will be sufficient for this patient and the treatment plan will be switched to SBRT for the remaining fractions. Otherwise, the patient will complete the standard fractionation.

Twelve intermediate-risk prostate cancer patients who received standard radiotherapy were identified to investigate the feasibility of this strategy. An institutional REB exemption was granted. Three margins were used in the

SBRT re-plan: 5 mm isotropic, 5 mm in all directions except 4 mm and, 3 mm posteriorly. Reconstructed CTV dose (D95%, D98%) were compared against the planned dose (CTV/PTV D95%, PTV D98%). The plan identified with maximal coverage while minimizing dose to organs at risk in the first 4 fractions was copied onto fractions 8, 12, 16, and 20 for validation of CTV coverage.

RESULTS

Ten cases met PACE-B protocol using 5 mm (3 cases), 4 mm (4 cases), and 3 mm (3 cases) posterior margins. The volume of rectum encompassed by PTV (inRectum) and the ratio of inRectum to PTV were shown to potentially predict whether a 5 mm-margin SBRT plan could be achieved.

To date, dose reconstruction has been performed for one 5 mm-margin case on all 8 fractions of CBCT. Reconstructed CTV dose (D95%, D98%) exceeded PTV planning dose in all fractions. As expected, CTV D95% decreased from CTV planning dose: range [-0.3%, -3.1%] in the first 4 fractions and [0.1%, -1.1%] in the 4 validation fractions.

CONCLUSION

Preliminary results suggest that it may be feasible to use the proposed strategy with 5 mm PTV margins, without the need for fiducials or rectal spacers. Completed dose reconstruction on all cases will determine whether smaller PTV margins are feasible for this strategy.

08 Your Voice Matters During Covid-19: Evaluation of Digital Divides Across a Tertiary Cancer Centre

Amir Safavi, Mike Lovas, Damon Pfaff, Zhihui Amy Liu, Sheena Melwani, Shayla Devonish, Tran Truong, Nazek Abdelmutti, Danielle Rodin, Alejandro Berlin

PURPOSE

Virtual care (VC) and electronic patient-reported experience measures (ePREM) have been systemically adopted during the COVID-19 pandemic to facilitate continuity of cancer care and quality improvement. Digital divides, defined as differential access and benefit from these tools, may exacerbate existing health inequities among patients. We aimed to evaluate digital divides through ePREM access, use, and responses during the pandemic.

METHOD

Your Voice Matters (YVM), a provincially-mandated ePREM survey, was adapted to an online platform in September 2020 and emailed to patients after outpatient VC and in-person clinic visits at a tertiary cancer centre in Ontario. Patient age, gender, postal codes, and completed surveys from September-December 2020 were collated. Income was estimated using area-level averages from Statistics Canada 2016 census data. Socioeconomic status was mapped to area-level dimensions of the Canadian Index of Multiple Deprivation: residential instability (RI), economic dependency, ethnocultural composition (EC), situational vulnerability (SV). Higher factor scores per dimension correspond to greater marginalization. Two-sided Chi-squared and t-tests were used to compare demographics between VC and in-person patients with a significance threshold of $p < 0.001$. Generalized estimating equations logistic regression models were used to assess associations between patient satisfaction and visit type, as well as demographics.

RESULTS

YVM was emailed to 28% (10625/37835) of patients with a response rate of 21.8% (2321/10625). Mean and minimum income (x \$10,000) were highest among responders (6.6, 1.5) compared to non-responders (6.3, 1.3) and those without email (6.2, 1.1). Comparing responders with VC (n=549) and in-person (n=1719) visits, the former had higher mean income (6.9 vs 6.5, $p < 0.001$) and lower mean EC factor score (0.2 vs 0.4, $p < 0.001$). Satisfaction with care received was not associated with visit type and satisfaction with VC logistics was not associated with demographics. Patients with higher EC scores were more likely to rate low satisfaction in the “culturally appropriate” (OR 0.69, 95% CI: 0.57-0.85) domain. Patients with higher SV scores were more likely to rate low satisfaction in the “physical symptoms” (OR 0.69, 95% CI: 0.51-0.94) domain, while patients with higher RI scores were more likely to rate low satisfaction in the “physical” (OR 0.82, 95% CI: 0.69-0.98) and “emotional symptoms” (OR 0.88, 95% CI: 0.79-0.98) domains.

CONCLUSION

VC patients had positive experiences with visit logistics across demographics and their satisfaction with care was comparable to that of in-person patients. However, VC use and ePREM access, use, and responses were associated with income and socioeconomic status. Identifying populations vulnerable to digital health inequities will guide strategies to bridge the divides.

09 Surgical Resection(s) Plus Stereotactic Radiosurgery (SRS) Versus SRS Alone for Large Brain Metastases: A Comparative Study

Enrique Gutierrez, Barbara-Ann Millar, Normand Laperriere, Tatiana Conrad, Aristotelis Kalyvas, Gelareh Zadeh, Mark Bernstein, Paul Kongkham, Jessica Weiss, David Shultz

PURPOSE

Large brain metastases (BM) are challenging to manage. Therapeutic options include SRS or surgery (S) plus SRS. We sought to compare the following outcomes: overall survival (OS), local failure (LF), radionecrosis (RN), pachymeningeal (PM) and leptomeningeal (LM) in patients treated with Gamma Knife (GK) SRS alone vs S+SRS.

METHOD

We reviewed a prospective registry database of BM patients treated from 2008 to 2019. All patients at least 18 years old with large BM (≥ 4 cc in volume) treated with SRS or S+SRS were included in this analysis. Exclusion criteria included the absence of post-treatment follow-up. WBRT or SRS targeting the index lesion were censoring events. Survival percentages were calculated using the Kaplan-Meier method. Differences between groups were tested using the Cox proportional hazards model. Other outcomes were calculated using the cumulative incidence method.

RESULTS

383 BM patients were identified, 128 and 255 were treated with S+SRS and SRS, respectively. Median ages in the S+SRS and SRS groups were 62.2 (23.6-98.5) and 60.2 (20.2-97.4), respectively (P 0.33). Median target volumes for S+SRS and SRS were 15.1cc (4-54) and 6.5cc (4-36.9) (P < 0.001)

respectively. Median number of BMs treated concurrently with the index lesion for the S+SRS and SRS groups was 1 (1-10) and 2 (1-11), respectively (P < 0.001). OS at 12 and 24 months was 69% and 41% vs 55% and 20% for the S+SRS and SRS groups, respectively hazard ratio (HR) 1.64 (1.23-2.18) (P < 0.001). Cumulative incidence of LF requiring salvage surgery at 12 and 24 months were 3% and 5% vs 8% and 10% for S+SRS and SRS groups, respectively (P 0.067). Incidence of RN at 12 and 24 months were 9%, and 17% vs 15%, 21% for S+SRS and SRS groups, respectively 1.32 HR (0.77-2.29) (P 0.32). Cumulative incidences of PM disease at 12 and 24 months were 16% and 21% vs 3% and 7% for S+SRS and SRS groups, respectively HR 0.26(0.12-0.56) (P < 0.001). Cumulative incidences of LM disease at 12 and 24 months were 4% and 6% vs 2% and 4% for S+SRS and SRS groups, respectively HR 0.73(0.25-2.17) (P 0.57).

CONCLUSION

In this series, the addition of S to SRS correlated with improved OS and a trend towards a lower incidence of LF compared to SRS alone. However, patients treated with S showed an increased risk of PM failure.

10 An Articulated Robot for In-bore Sequential Needle Insertion under MRI-Guidance

Amanda Aleong, Thomas Looi, Satwinder Singh, Kevin Luo, Alejandro Berlin, Michael Milosovic, James M. Drake, Robert Weersink

PURPOSE

Percutaneous needle-based interventions such as transperineal prostate brachytherapy require the accurate placement of multiple needles to treat cancerous lesions within the target organ. To guide needle placement, magnetic resonance imaging (MRI) offers excellent visualization of the target lesion without the need for ionizing radiation. To date, multi-needle insertion relies on a grid template which limits the ability to steer individual needles. This work describes an MR-compatible robot designed for the sequential insertion of multiple needles under MR guidance. This strategy presents a novel approach, enabling the robot to maneuver around existing needles while minimizing the footprint of the robot.

METHOD

The 6-DOF system is designed with an articulated arm to extend the reach of the robot. The impact of the robot on image quality was tested for four sequences (T1w-TSE, T2w-TSE, VIBE and BEAT) on a 1.5T Siemens Magnetom Aera. The joint-level uncertainty was measured by repeatedly driving each joint over a set distance for a range of available joint values. A magnetic seed was fixed to the base of the joint and tracked using an NDI Aurora magnetic tracker. Each joint was driven back and forth, 10 times in each direction. The mean error and standard deviation for each joint and distance was calculated. The feasibility of sequential needle insertion was validated in a gelatin phantom. The phantom was marked with four insertion points on the proximal face of the phantom. The robot was driven

to each target position in the order shown in the diagram by entering appropriate joint values with the needle guide closed. At each position, a needle was inserted orthogonal to the surface of the gel phantom. The needle was then released by opening the needle guide and the process was repeated for the other three entry points.

RESULTS

Quantification of the signal-to-noise ratio showed 29% maximum signal loss in a saline phantom when the system was powered on. Joint level testing showed a maximum error of 2.47 ± 0.41 Degrees for revolute joints and 0.68 ± 0.33 mm for prismatic joints. The theoretical workspace spans the proposed clinical target surface of 10 x 10 cm. Lastly, the feasibility of multi-needle insertion was demonstrated with four needles successfully placed in a gelatin phantom.

CONCLUSION

The robot described in this work supports multi-needle insertion under real-time MR-guidance. The implementation of a robotic system equipped with real-time MRI feedback has the potential to improve the safety and efficiency of MR-guided percutaneous procedures such as prostate brachytherapy. This approach may be used to overcome specific challenges in the clinic such as deflection due to non-linear needle-tissue interactions, lack of in-bore access to the patient and safety concerns regarding robotic operation.

11 **ATM Inhibitor AZD1390 Radiosensitization as a Strategy to Enhance Innate Immune Activation in Small Cell Lung Cancer (SCLC) Cell Lines and Syngeneic Genetically-Engineered Mouse Models (GEMM)**

Xiaozhuo Ran, Benjamin Lok

PURPOSE

Aim 1: Determine the radiosensitization and synergistic innate immune activation by AZD1390 in SCLC cell lines.

Aim 2: Investigate the mechanism of synergistic innate immune activation by AZD1390 and RT.

Aim 3: Demonstrate radiosensitization, innate immune activation, and immunotherapy response (anti-PDL1) in immune competent GEMM allograft models of SCLC.

METHOD

We used cell viability assay and clonogenic assay to evaluate the radiosensitization by AZD1390. Also, we used comet assay and micronuclei staining to assess DNA damage by AZD1390+RT. Besides, we assessed the innate immune activation by quantitative RT-PCR and immunofluorescence. Last, we will measure the anti-tumor efficacy and immune profiling in GEMM model by flow cytometry.

RESULTS

We demonstrated that AZD1390 sensitizes cell response to RT by cell viability assay and clonogenic assay. Results from comet assay and micronuclei staining showed that the radiosensitization by AZD1390 is due to increased DNA damage and decreased genomic stability. Meanwhile, the quantitative RT-PCR showed that the increased DNA damage leads to the translocation of cGAS and subsequent innate immune activation, including ccl5 and cxcl10 increased expression.

CONCLUSION

ATM inhibitor AZD1390 sensitizes cell response to RT and enhances innate immune activation in small cell lung cancer.

12 Excessive Transcription-Replication Conflicts are a Vulnerability of BRCA1-Mutant Cancers

Parasvi S. Patel, Arash Algouneh, John J. Reynolds, Jihoon Lee, Yue Feng, Chehronai Fozil, Talya Yerlici, Luis Palomero, Fraser Soares, Musa Ahmed, Anne Hakem, Karim Mekhail, Miquel Angel Pujana, Grant S. Stewart, Hansen He, Razq Hakem

PURPOSE

The breast cancer susceptibility gene 1 (BRCA1) gene encodes tumor suppressor BRCA1, which primarily functions to maintain genomic stability. BRCA1 is a critical component of various multi-protein complexes that allow error-free repair of double-stranded DNA breaks through homologous recombination (HR). BRCA1 also plays a crucial role in cell cycle regulation, as well as and transcriptional and epigenetic regulation. Given its role in maintaining genomic integrity, it is not surprising that mutations in the BRCA1 gene increase the risk of developing breast, ovarian, and other cancers. Additionally, patients suffering from BRCA1-defective cancers are likely to experience poor clinical outcomes due to relapse, metastasis, and the development of a new contralateral tumor in the years following diagnosis. Therefore, identifying novel therapeutic targets that explicitly eliminate tumors that arise from BRCA1 mutations is of utmost importance.

METHOD

Using a targeted CRISPR/Cas9 drop-out screen, we identified proteins whose loss negatively affects viability of BRCA1-mutant breast and ovarian tumors. We examined the hits identified in our drop-out screen in a BRCA1-deficient setting using cell-based assays, immunoprecipitation (IP), chromatin IP (ChIP), immunofluorescence, western blotting, and DNA-RNA IP (DRIP) assays.

RESULTS

Our CRISPR-Cas9 dropout screen identified Methylphosphate Capping Enzyme, MePCE, as a potential synthetic lethal interactor of BRCA1. Mechanistically, depletion of MePCE in a BRCA1-deficient setting results in increased transcription stress, R-loop accumulation, as well as replication stress concomitantly contributing to transcription-replication collision events. These factors compromise genomic integrity, thereby resulting in loss of viability of BRCA1-deficient tumors. We also identified RNA polymerase II-associated factor I, PAF1, as a synthetic lethal interactor of BRCA1. Similar to MePCE depletion, loss of PAF1 in a BRCA1-deficient setting results in R-loop accumulation, transcription-replication conflicts, and cell death.

CONCLUSION

Our study highlights the dependence of BRCA1-defective tumors on factors such as MePCE and PAF1 that suppress transcription-replication conflicts through PolII pausing and release regulation to maintain genomic stability and highlights the untapped potential of these factors as novel therapeutic targets for the treatment of cancer associated with BRCA1 mutations.

13 Dose Accumulation Comparison Between Adapt-to-Shape and Adapt-to-Position for MRL Adaptive SBRT Prostate Treatments at the Princess Margaret Cancer Centre

*Christopher D. Johnstone, Tony Tadic, Victor Malkov,
Daniel Letourneau, Jeff Winter*

PURPOSE

To use dose accumulation to directly compare two strategies for online adaptation on an MR-Linac (MRL): the adapt-to-position (ATP) isocentric shift approach versus the full re-optimization adapt-to-shape (ATS) approach for prostate SBRT treatment.

METHOD

This study analyzed 12 prostate SBRT patients treated at our centre with 30 Gy in 5 fractions on a 1.5 T MRL using 9-field IMRT with MR-based reference planning. The ATP workflow adapts beams following translation-only rigid registration of the prostate. The ATS workflow generates a new treatment plan to match the daily anatomy using deformable image registration (DIR) and manual online contour editing by a Radiation Oncologist. Treatment plans on the localization MR images were created for all fractions using both ATP (simulated) and ATS (clinical) workflows. All plans were imported into a commercial treatment planning system to perform DIRs and accumulate dose on the reference MR images. Clinical goal DVH metrics for accumulated ATP and ATS dose distributions were compared with Student's t-tests.

RESULTS

Mean (\pm STD) CTV D98 was not significantly different between ATP (3132 ± 129 cGy) and ATS (3180 ± 90 cGy), and satisfied the > 2850 cGy clinical goal for 11 of 12 patients for ATP and all patients for ATS. DVH goals for femurs (D5 < 1200 cGy), rectum (D1cm3 < 3000 cGy, D20 < 2000 cGy, D50 < 1000 cGy) and bladder (D5cm3 < 3000 cGy) were not significantly different between ATP and ATS. Organ-at-risk clinical goals were not met in 6 patients (12/72 goals) for ATP and 2 patients (3/72 goals) for ATS.

CONCLUSION

Salvage MRgHDBT was a safe and well-tolerated treatment with minimal adverse effects on urinary and bowel QoL measures but detrimental to sexual QoL. Further analysis with larger sample size might clarify the complex relationship between implant characteristics, dose-volume, toxicity and QoL.

14 A Cross-Voxel Exchange Model for The Estimation of Kinetics Parameters of Tumour Tissue

Noha Sinno, Tord Hompland, Ed Taylor, Michael Milosevic, David Jaffray, Catherine Coolens

PURPOSE

The efficient delivery of drugs to tumours is essential for an enhanced response to treatment. Research highlights the connection between tumour perfusion parameters and tumour progression and treatment outcome. Transport models, when combined with DCE-MRI, can provide insight into the microenvironmental properties of tumours. The Cross-Voxel Exchange Model (CVXM) incorporates cross-voxel exchange and allows a comprehensive estimation of kinetic parameters of tumour tissue (convection, diffusion and extravasation). It is employed in preclinical models to estimate metrics relating to the aforementioned three transport mechanisms.

METHOD

CVXM was fitted to twenty TS-415 human cervical carcinoma xenografts resulting in spatial maps for fluid flow velocities v , diffusion coefficients D , extravasation rate K_{ext} and extra-cellular extra-vascular volume fraction of tissue v_e . The xenografts were established inside the gastrocnemius muscle of adult female BALB/c nu/nu mice. After injection with Gd-DTPA, the mice were subjected to DCE-MRI for a period of 15 minutes at a spatial resolution of $0.23 \times 0.23 \times 2.0 \text{ mm}^3$ and a time resolution of 14 seconds. Regions of interests were selected radially from the tumour center outwards. The fitted parameters v , D , K_{ext} and v_e were constrained between $[0, 20] \mu\text{m/s}$, $[0, 1000] \mu\text{m}^2/\text{s}$, $[0, 10] \text{ min}^{-1}$, and $[0, 1]$ respectively.

RESULTS

Examining the MRI scans, tumours were categorized into two groups: (A) nine are round and (B) eleven tumours have a lobulated shape. Group (B) exhibited higher velocity measures at the periphery than group (A) did. All tumours presented a faster and higher tracer uptake at their periphery. The tumour centers were also perfused but at a slower pace.

CVXM permitted the derivation of the perfusion parameters for diffusion, convection and extravasation: velocity measures at the periphery average to $14.37 \pm 3.65 \mu\text{m/s}$, mean D , K_{ext} and v_e are $253.98 \pm 85.37 \mu\text{m}^2/\text{sec}$, $0.02 \pm 0.01 \text{ min}^{-1}$ and 0.09 ± 0.02 respectively. The higher velocities at the periphery explain the high enhancements in that area. The slower concentration uptake towards the center of the tumour can be associated with the slower acting diffusion of tracer in tissue.

CONCLUSION

CVXM, when paired with DCE-MRI, allows the distinction between the three transport processes governing drug delivery. Higher fluid flow velocities were found at the tumour periphery for all xenograft cases which could hinder drug distribution to the tumour center but smaller particles can still diffuse to that area over a longer period of time. The preclinical findings promise an enhanced personalized treatment planning.

15 Physician and Patient Reported Morbidity After MR-Guided Salvage Brachytherapy for Prostate Cancer

Inmaculada Navarro, Lisa Joseph, Amy Liu, Alejandro Berlin, Joelle Helou, Srinivas Raman, Robert Weersink, Alexandra Rink, Bernadeth Lao, Cynthia Ménard, Peter Chung

PURPOSE

Local salvage brachytherapy (BT) after previous radical radiotherapy (RT) in prostate cancer (PC) may cause additional toxicities that negatively impact quality of life (QoL). We report on QoL for patients treated in a prospective study.

METHOD

From 2009 to 2020, 50 PC patients underwent 2 fractions of MR-guided HDR salvage BT (MRgHDRBT) for locally recurrent disease after RT in 2 non-randomized cohorts. Cohort 1 whole gland treated with total 16Gy with an integrated boost (wgBT) of 22Gy to GTV. Cohort 2 focal HDR (fBT) to total 26Gy. GTV was defined on multiparametric MRI. For wgBT the GTV-PTV expansion was 2mm except 4 mm superior-inferior (s/i). For fBT, GTV-CTV expansion was 5 mm restricted to within 2 mm of the prostate and PTV of 2 mm s/i. Toxicity was assessed using CTCAE v4 and the Expanded Prostate Cancer Index Composite (EPIC) for QoL at baseline and after HDR. Multivariable linear regression model accounting for repeated measurements within individual and adjusting for baseline score and time was fitted to compare cohorts and to assess association between dosimetry and QoL.

RESULTS

The median age was 71 (range 62,85) with a median follow-up of 60.5 (6,134) months. Thirty-seven (74%) patients had fBT, and 13 (26%) wgBT. The median GTV-PTV volume, was 7 cm (3.6,18.4) and 7.5 cm (3.2,16.4) per fraction in fBT; compared with 3.4 cm (1.1,8.5) and 4.1 cm (0.9, 8) in wgBT. These volumes received a median PTV V100 of 98% in fBT and 100% in wgBT. The median dose D0.5 cc in fBT compared to wgBT was 8.4Gy vs. 9.5Gy for the urethra, 5.4Gy vs. 7Gy bladder and 8.6Gy vs. 7.3Gy rectum.

The 5-year biochemical control was 45.2% (95% CI 31.5, 64.9). There was no G3 toxicity. In the fBT group 23 (62%) patients had grade 1 GU toxicity, and 2 (5%) G2; compared with 5 (38%) and 8 (62%) in the wgBT cohort, respectively. Grade 1 GI toxicity developed in 4 (11%) with no G2 after fBT, whereas in the wgBT, 4 (31%) and 3 (23%) reported G1 and G2 GI toxicity. A minority of 17 (34%) men had adequate sexual function before salvage BT of whom 6 (35%) developed G1 toxicity and 3 (17.6%) developed G2 (5 and 1 patient in fBT group, respectively).

Scores in QoL demonstrated a decrease at month 1 which recovered by month 3 and was stable for urinary ($p < 0.001$) and bowel ($p = 0.013$) while sexual function continued declining during follow-up; with higher scores for fBT ($p = 0.018$).

CONCLUSION

Salvage MRgHDRBT was a safe and well-tolerated treatment with minimal adverse effects on urinary and bowel QoL measures but detrimental to sexual QoL. Further analysis with larger sample size might clarify the complex relationship between implant characteristics, dose-volume, toxicity and QoL.

16 Validation of The Truebeam Electron Monte Carlo Model Under Heterogeneous Tissue Conditions

Reza Askari, Xia Wu

PURPOSE

In many clinical scenarios in radiation oncology, irregular surface shapes and tissue heterogeneities, such as air cavities and bones may lead to uncertainties in predicting dose delivered by electron beams, and thus impacting target coverage and OAR sparing. Monte Carlo (MC) simulation is the leading algorithm for accurate electron beam dose calculation, which accounts for contours, tissue densities (i.e., patient anatomy), and irradiation geometry. The electron Monte Carlo (eMC) dose calculation algorithm in the Varian Eclipse system is a fast implementation of the macro Monte Carlo for calculation of dose from high-energy electron beams. The purpose of this study is to examine the accuracy of the dose distribution prediction of Eclipse eMC for irregular surface shapes and heterogeneous tissue settings.

METHOD

A tissue-equivalent anthropomorphic phantom, adult male ATOM 701D from CIRS, was scanned using a Philips 16 slice big bore CT in 2mm slice thickness. Custom cut GafChromic EBT3 film dummies were sandwiched in the slabs of the phantom in the region of interests and the slabs were tightened during CTsim to minimize the air gap between the phantom and the films. Electron plans mimicking clinical treatment scenarios were generated in Eclipse, and calculated using eMC version 13 with a grid size of 0.15cm. The eMC V 13 model had been previously validated under homogeneous water equivalent settings with planar surface. The anthropomorphic phantom with EBT3 films sandwiched in between was then set up on the treatment couch according to the plan and the electron

plans were delivered using a Varian Truebeam LINAC. The films were analyzed using filmQA pro V 4.0 software and doses were compared to Eclipse calculation to observe any discrepancies. The film calibrations were done in dose ranges of 0 to 300cGy using the same Varian Trubeam linac. The calibration curve for each energy was also generated using FilmQA pro v 4.0. So far, the region of interests we have selected including the nose, slabs 5-6 and the sternum, slabs12-13. The beam was defined by a 10x10 cm² applicator with a standard 10x10 cutout of various SSD, and a gantry angle of 0°. If time permit, we planned to use an in-house-built true electron Monte Carlo calculation algorithm to help us understand the source of the discrepancy between the Eclipse calculations and film results.

RESULTS

Two sets of film measurements have been performed so far for the nose plan and one for the sternum. Large discrepancies of over 10% were observed between eMC dose calculations and measurements in both depth-dose curves and beam profiles for both 9 and 12MeV. The discrepancies were observed near the edges of the phantom in regions with large surface curvature, e.g. in the nose region. In general, the greatest discrepancies occur in the gradient regions at lower energies. Investigations are ongoing to validate the approach.

CONCLUSION

Eclipse eMC dose calculation was evaluated under heterogeneous tissue setting and irregular surface shapes. The validation of the methodology is ongoing.

17 Patient-derived Xenograft Engraftment Predicts Oral Cavity Cancer Outcomes

Badr Id Said, Laurie Ailles, Christina Karamboulas, Jalna Meens, Shao Hui Huang, Wei Xu, Sareh Keshavarzi, Scott V. Bratman, B.C. John Cho, Meredith Giuliani, Ezra Hahn, John Kim, Brian O'Sullivan, Jolie Ringash, John Waldron, Anna Spreafico, John R. de Almeida, Douglas B. Chepeha, Jonathan C. Irish, David P. Goldstein, Andrew Hope, Ali Hosni

PURPOSE

Patient-derived xenografts (PDX) can help identify oral cavity squamous cell carcinoma (OSCC) patients at risk for disease recurrence and optimize clinical decision-making. In this study, we develop and validate a prediction score for locoregional failure (LRF) and distant metastases (DM) in OSCC that incorporates PDX engraftment in addition to known clinicopathological risk factors.

METHOD

PDX models were generated from OSCC patients. Patients were scored as a “non-engrafter” if PDX formation did not occur within 6 months. Multivariable analysis (MVA) was used to identify predictors of LRF and DM. Factors retained in the final MVA were used to construct a prediction score and classify patients into risk groups using a 10-fold cross-validation approach.

RESULTS

Overall 288 OSCC patients were analyzed. MVA identified pT3-4, pENE, and engraftment as predictors of LRF and DM. Patients whose tumours engrafted (n=198) were more likely to develop LRF (HR 1.98, 95% CI: 1.24-3.18, $p < 0.01$), and DM (HR 2.64, 95% CI 1.21-5.75, $p < 0.01$) compared to

non-engrafters. A prediction score based on the aforementioned variables identified patients at high-risk (defined as having at least two of the three high risk features i.e. engraftment, pT3-4, pENE) and low-risk for LRF (43.5% vs 26.5% at 5-years, $p < 0.001$), DM (38.2% vs 8.4% at 5-years, $p < 0.001$), and poorer 5-year OS (34% vs 66%, $p < 0.001$). The prediction model that included engraftment had the highest discriminatory capacity in the cross-validation analysis (AUC: 67.8 [63.5-72.9]), while removal of engraftment as a predictor resulted in a lower c-index (AUC: 62.7 [57.0-68.4]). In patients classified based on a clinical score only (i.e. presence or absence of pT3-4 and pENE), engraftment remained useful in identifying those with worse outcomes. Compared to non-engrafters, engraftment was associated with higher rates of DM (15.8% vs. 5.4%, $p < 0.05$) in clinically “high risk” patients as well as higher rates of LRF (31.9% vs. 13.8%, $p < 0.05$) in clinically “low risk” patients at 5-years. Finally, engraftment was associated with poorer 5-year OS in both clinically “high risk” (36% vs. 65%, $p < 0.05$), and “low risk” patients (57% vs. 78%, $p < 0.01$).

CONCLUSION

A prediction score utilizing OSCC PDX engraftment, in conjunction with pT3-4 and pENE, improves the prognostic utility of existing clinical models and predicts patients at risk for LRF, DM and poor survival.

18 Re-evaluating Surgery and Re-irradiation for Locally Recurrent Pediatric Ependymoma – A Multi-Institutional Study

David Y. Mak, Normand Laperriere, Vijay Ramaswamy, Eric Bouffet, Jeffrey C. Murray, Rene Y. McNall-Knapp, Kevin Bielamowicz, Arnold C. Paulino, Wafik Zaky, Susan L. McGovern, M. Fatih Okcu, Uri Tabori, Peter B. Dirks, Michael D. Taylor, Derek S. Tsang, Abhishek Bavle

PURPOSE

The goal of this study was to evaluate extent of surgical resection, and timing and volume of re-irradiation, on survival for children with locally recurrent ependymoma.

METHOD

Children with locally recurrent ependymoma treated with a second course of fractionated radiotherapy (RT2) from six North American cancer centres were reviewed. The index time was from the start of RT2 unless otherwise stated.

RESULTS

35 patients were included in the study. The median doses for first radiation (RT1) and RT2 were 55.8 and 54 Gy, respectively. Median follow-up time was 5.6 years. Median overall survival (OS) for all patients from RT2 was 65 months. Gross total resection (GTR) was performed in 46% and 66% of patients prior to RT1 and RT2, respectively. GTR prior to RT2 was independently associated with improved PFS for all patients (HR 0.41, $p = 0.04$), with an OS benefit (HR 0.26, $p = 0.03$) for infratentorial tumours.

Median PFS was superior with craniospinal irradiation (CSI) RT2 (not reached) compared to focal RT2 (56.9 months; log-rank $p = 0.03$). All distant failures (except one) occurred after focal RT2. Local failures after focal RT2 were predominantly in patients with less than GTR pre-RT2.

CONCLUSION

Patients with locally recurrent pediatric ependymoma should be considered for re-treatment with repeat maximal safe resection (ideally GTR) and CSI re-irradiation.

19 Impact of the COVID-19 Pandemic on Radiotherapy Patterns of Practice for Curative Intent Breast Cancer Patients

Donna Liao, Kawalpreet Singh, Joelle Helou, Anthony Fyles, Ezra Hahn, Kathy Han, Naghmeh Isfahanian, Danielle Rodin, Aisling Barry, Fei-Fei Liu, Grace Lee, Amy Liu, Srinu Raman, Alejandro Berlin, Michael Milosevic, Anne Koch, Jennifer Croke

PURPOSE

In response to the COVID-19 pandemic, radiotherapy (RT) departments around the world created new policies as a means of reducing risk of exposure for patients and staff, while attempting to maintain high-quality RT. We aim to describe the impact of the pandemic on changes in breast cancer RT patterns of practice for new patient referrals at a tertiary cancer center.

METHOD

Newly diagnosed breast cancer patients referred to our department from March 17-June 30, 2020 were included. Referrals for palliative RT were excluded. Demographic characteristics, COVID-19 status (if available) and RT treatment information, including deviations from usual practice because of the pandemic, were extracted from medical records by independent reviewers, and validated by the treating radiation oncologist. Descriptive statistics were used to summarize the data. The results were compared to breast cancer patients treated from March 17-June 30, 2019.

RESULTS

A total of 271 and 306 patients met selection criteria for the 2020 and 2019 cohorts, respectively. The majority of consultations in 2020 were virtual (96%), conducted via telephone, OTN or MS Teams, whereas in 2019 all

were conducted in-person. Median age of the cohorts was similar: 58 years (range: 24-86) in 2020 and 59 years (range: 26-88) in 2019. Of those treated with adjuvant RT (n=209), 56% of patients received whole breast (WB), 36% regional nodal irradiation (RNI) and 8% partial breast (PB) RT in 2020, whereas in 2019 (n=284), 60% received WB, 31% RNI and 9% PB (Chi-squared test p=0.43). As a result of the pandemic, 78% of cases (n=211) received one or more deviations in RT practice compared to pre-pandemic institutional policies. The most common was an “altered dose/fractionation protocol” (n=197; 93%), such as use of hypofractionated RNI (2020: 97%, 74/76 cases vs. 2019: 3%, 3/87 cases) or the FAST Forward regimen (2020: 43%, 57/134 WB/PB cases vs. 2019: 0/197 cases). Other deviations included a delay in RT start (defined as >12 weeks post-op) noted in 11% (n=29) and omission of RT in only 8% (n=17), both were recommended when the risks associated with COVID-19 were felt to outweigh the benefit of RT. One patient had a deviation in RT as a result of testing positive for COVID-19.

CONCLUSION

In order to minimize hospital visits in response to the COVID-19 pandemic, a substantial proportion of breast cancer patients were seen virtually and treated with newer hypofractionated dose schedules, while total omission of adjuvant RT was infrequently observed. Continuously tracking patterns of practice provides an opportunity to evaluate the impact of the pandemic on clinical outcomes and help inform post-pandemic value-enhancing practices.

20 Association of Tumour volume and outcomes in T3 Larynx cancer with organ preservation approach

Nauman Malik, Nicolin Hainc, Gia Gill, Steven Nakoneshny, Paul Kerr, Wayne Matthews, Adam Globerman, Joseph C. Dort, Pejman Maralani, Eugene Yu, John Lysack, Ali Hosni, Irene Karam, Antoine Eskander

PURPOSE

Organ preservation approaches in the treatment of locally advanced larynx cancers are widely used and consist of radiotherapy (RT) with or without concurrent systemic therapy (CRT). Analyses of the National Cancer Database suggest that at the population level, survival in this disease may be decreasing, as CRT became more widely adopted in lieu of total laryngectomy (TL). Tumor volume in T3 laryngeal tumors has been hypothesized as a variable to explain this finding, with higher volume associated with lower local control, though largely in the pre-intensity modulated radiotherapy (IMRT) era. The purpose of this study was to analyze outcomes for T3 laryngeal cancer treated with IMRT.

METHOD

This was a national, multicentre retrospective cohort study of patients diagnosed with American Joint Committee on Cancer (AJCC) T3 N0-3 M0 glottic and supraglottic cancers who underwent curative intent IMRT with or without systemic treatment from 2002-2018. Tumor volumes were calculated using a validated standardized approach by a Neuroradiologist. Primary predictor was tumor volume, primary outcome was local control (LC), and secondary outcomes included overall survival (OS), as well as late grade ≥ 3 toxicities. Kaplan Meier estimates and log-rank tests were used for

survival analyses, with Cox proportional hazards used for univariable analyses.

RESULTS

246 patients met inclusion criteria, 147 glottic and 99 supraglottic cancers. At baseline, glottic patients were more likely to be male (87% vs 74%, $p < 0.01$), have a fixed vocal cord (63% vs 39%, $p < 0.01$), not have pre-epiglottic space invasion (6% vs 34%, $p < 0.01$), be cN0 (83% vs 40%, $p < 0.01$), and have lower grade tumors (20% vs 7%, $p < 0.01$). Mean tumor volumes for glottic and supraglottic tumors were 5.0 (4.2-5.8) cc and 13.0 (10.3-15.6) cc respectively. Univariable analysis showed systemic therapy was associated with improved local failure (HR 0.49, 95%CI 0.24 – 0.99, $p = 0.05$). Within the glottic cohort, tumor volume was not associated with local failure (HR 1.09, 95%CI 0.71 – 1.67, $p = 0.38$), however having a local failure event was associated with increased feeding tube dependence (HR 2.52, 95%CI 1.05 – 6.02, $p = 0.04$). Median local failure free survival in the overall cohort was 28.5 months, with median OS 23.2 months. There was a trend towards improved local control in the supraglottic cohort compared to glottic patients (log-rank $p = 0.08$), but the supraglottic cohort had significantly worse overall survival (log-rank $p = 0.02$).

CONCLUSION

In this retrospective cohort study, there were baseline and outcome differences between patients with T3 glottic and supraglottic larynx cancer, with worse overall survival in supraglottic patients. Tumor volume was not associated with local control in the glottic cohort. These findings are pending further validation in a larger cohort and will be analyzed separately for supraglottic tumors.

21 Feedback Delivery in an Academic Cancer Centre: Reflections from an R2c2-Based Microlearning Course

Amir Safavi, Janet Papadakos, Tina Papadakos, Naa Kwarley Quartey, Karen Lawrie, Eden Klein, Sarah Storer, Jennifer Croke, Barbara-Ann Millar, Raymond Jang, Andrea Bezzak, Meredith Giuliani

PURPOSE

Feedback delivery and training have not been characterized in the context of academic cancer centres. The purpose of this study was to assess the feasibility and utility of a microlearning course based on the R2C2 (Relationship, Reaction, Content, Coaching) feedback model and to characterize multidisciplinary staff perspectives on existing feedback practices in an academic cancer centre.

METHOD

A prospective longitudinal qualitative design was utilized. Five staff (two radiation oncologists, one medical oncologist, and two allied health professionals) with supervisory roles were selected by purposive sampling. The course, consisting of a web-based multimedia module, was completed by each participant. Semi-structured one-on-one interviews were conducted with each participant at four time points: pre- and immediately post-course, and at one- and three-months post course. Interviews were audiotaped and transcribed verbatim. An abductive approach informed by the R2C2 model was used to code transcripts and generate themes.

RESULTS

All participants found the course to be time feasible and completed it in 10-20 minutes. The course was deemed useful by participants and fulfilled their self-reported needs for feedback training and normalization of feedback culture in the cancer centre. Learning retention of the R2C2 model was present in four of five participants at three-months post course. The “relationship building” and “exploring reactions” domains facilitated the most reflection during post-course interviews. Three relationship-oriented themes were identified regarding perceptions of existing feedback practices: 1) hierarchical and interdisciplinary relationships modulate feedback delivery, 2) interest in feedback delivery varies by duration of the supervisory relationship, and 3) the transactionality of supervisor-trainee relationships influences feedback delivery.

CONCLUSION

Conclusion: An R2C2-based microlearning course is time feasible and useful to the multidisciplinary study participants. The impacts of current feedback practices and R2C2 on recipient learning and clinical performance require further study.

22 Prostate SBRT on the MR-Linac at Odette Cancer Centre: Is the Longer Time Required In MRI-Guided Online Adaptation Prostate SBRT Justified?

Eyesha Hashim-Younus, Andrew Loblaw, Patrick Cheung, William Chu, Chia-Lin Tseng, Danny Vesprini, Jay Detsky, Mikki Campbell, Melanie Davidson, Matt Wronski, Mark Ruschin

PURPOSE

Hypo-fractionated prostate SBRT performed on the MR-linac (MRL) with daily anatomical adaptation has already been demonstrated by our group to be dosimetrically superior to a rigid-shift based approach in terms of safely targeting disease. The aim of this work is to show that the prolonged treatment times required for online adaptive prostate SBRT are justified considering the improved patient-specific dosimetry.

METHOD

Our institution has to-date treated 28 prostate cancer patients on the MRL using 40 Gy in 5 fractions. The clinical target volume (CTV) is the prostate plus the proximal 1cm of seminal vesicles. During the online daily adaptation, the physician adjusts the anatomical contours on first localization MRI (“MR-loc”), followed by a plan re-optimization to adapt the reference pre-plan to the current anatomy (referred to as “adapt to shape”, or ATS). Just prior to treatment, a verification MRI (“MR-ver”) is acquired to ensure that the patient anatomy has not substantially changed during the adaptation process. Our clinical dosimetric goals (and tolerances) include: CTV volume receiving 40Gy greater than 99% (CTV V40Gy>99, tolerance>95); bladder V39.5Gy<2cm³ (tolerance<3cm³); rectum V38Gy<1cm³ (tolerance<1.5cm³) and maximum dose (Dmax) to rectum <40.6Gy (tolerance<42Gy); all of which have been shown to be related to patient

outcomes. We measured the dosimetric goals for 3 plans: (1) the treated ATS plan (ATS-loc); (2) an adapt to position (ATP) which is a shift-based approach retrospectively calculated on MR-loc (ATP-loc) and (3) ATS-loc re-calculated on MR-Ver (ATS-ver). The dosimetric goals were compared on a fraction-by-fraction basis for 6 patients (fractions=29) for ATS-loc and ATP-loc and for 2 patients (fractions=9) for ATS-ver. To study the net effects over all fractions, we accumulated the dose of all 3 plans over all fractions using deformable image registration for a subset of 2 patients.

RESULTS

The mean (+/- S.D.) time between MR-loc and MR-ver acquisitions (the time required for contouring and ATS re-planning) was 25 min (+/-5min). All ATS-loc fractional plans achieved CTV V40Gy>99, while only 1 ATP-loc and no ATS-ver plan achieved it.

The fraction of daily plans’ tolerance violations for organs at risk (OAR) were as follows:

Bladder V39.5Gy<2 cm³: ATS-loc=2/29, ATP-loc=10/29, ATS-ver=0/9;

Rectum V38Gy<1cm³: ATS-loc=2/29, ATP-loc=5/29, ATS-ver=1/9;

Rectum Dmax: ATS-loc=6/29, ATP-loc=14/29, ATS-ver=1/9.

Where dose accumulation was performed, the only OAR tolerance violation was in bladder for ATP-loc. The target coverage trended lower on MR-ver compared to MR-loc (mean: 93% versus 96%), but the difference was clinically irrelevant.

CONCLUSION

MR-guided online shape-adaptive plans improve dosimetry compared to conventional rigid position-adaptive plans. This dosimetric gain needs to be weighed against the longer times to deliver prostate SBRT fractions and in the future radiation side effects will be measured to determine if this dosimetric gain leads to an improvement in clinical toxicities.

23 Dosimetric Predictors of Toxicity and Quality of Life Following Single Fraction High Dose-Rate Prostate Brachytherapy

Mark Corkum, D. Andrew Loblaw, Hans Chung, Chia-Lin Tseng, Merrylee McGuffin, Melanie Davidson, Moti Paudel, Matt Wronski, Patrick Cheung, William Chu, Ewa Szumacher, Liying Zhang, Alexandre Mamedov, Gerard Morton

PURPOSE

Little is known about optimal dose constraints when high dose rate (HDR) brachytherapy is used as monotherapy for prostate cancer. Most dose constraints for HDR monotherapy were extrapolated from predictors of toxicity when HDR brachytherapy was combined with external beam radiotherapy as a boost. We sought to determine clinical and dosimetric predictors of toxicity and health related quality of life (HRQOL) in men treated with HDR brachytherapy as monotherapy.

METHOD

Eligible patients were treated with single fraction HDR brachytherapy as monotherapy on two prospective clinical trials at a single institution. Patients in the first trial (HDR-mono) received a single fraction of 19 Gy without a dominant intraprostatic lesion (DIL) boost, and patients from the second trial (MARS) received 19 Gy in a single fraction with an MRI-guided DIL boost to ≥ 23 Gy. ADT was not used. Univariable and multivariable logistic regression was used to evaluate clinical (age, IPSS score, prostate volume, alpha blocker use at baseline, and receipt of a DIL boost) and dosimetric (prostate V100, V150, V200, D90, Urethral Dmax and D10, and Rectal Dmax and V80) predictors of CTCAE v4 acute/late toxicity and HRQOL changes measured with expanded prostate index composite (EPIC). Three classifications of late minimally clinically important changes (MCICs) were

evaluated: small (>0.5 standard deviation [SD]), moderate (>1.0 SD) and severe (>2.0 SD) declines compared to baseline.

RESULTS

147 patients were included (87 from HDR-mono, 60 from MARS). Median follow-up was 62.8 months. Only increasing prostate size predicted acute GU toxicity \geq grade 2 (OR 1.05, 95% CI 1.01–1.09, $p = 0.021$). On multivariable regression, predictors of late GU toxicity \geq grade 2 were not receiving a DIL boost (OR 3.78, 95% CI 1.88–7.83, $p < 0.001$) and higher baseline IPSS score (OR 1.89, 95% CI 1.89–3.18, $p = 0.015$). Rectal and urethral dose constraints were not associated with late GU/GI toxicity \geq grade 2. Contrary to our hypothesis, small (OR 0.91, 95% CI 0.81–0.98, $p = 0.032$) and moderate (OR 0.91, 95% CI 0.80–0.98, $p = 0.037$) urinary MCICs were less frequent in those with higher urethral Dmax. No impact of urethra D10 on urinary MCICs was seen. Rectal Dmax and V80 did not predict bowel MCIC changes at any threshold.

CONCLUSION

Conclusion: We were unable to identify dose constraints that were predictive of late toxicity or relevant HRQOL changes in single fraction HDR brachytherapy. This suggests dose parameters used in these trials were safe, and that minor variability in plan dosimetry likely has little clinical significance. While increasing urethral Dmax paradoxically predicted for less frequent urinary MCICs, we do not believe this finding is clinically relevant. Further research exploring optimal dose constraints to be used in HDR brachytherapy as monotherapy for prostate cancer is warranted.

24 Limited-Stage Small Cell Lung Cancer: Outcomes Associated with Prophylactic Cranial Irradiation Over a 20-year Period at the Princess Margaret Cancer Centre

Tzen S. Toh, Michael Yan, Patricia Lindsay, Jessica Weiss, Katrina Hueniken, Christy Yeung, Vijithan Sugumar, Dixon Pinto, Tony Tadic, Alexander Sun, Andrea Bezjak, Johnathan Cho, Srinivas Raman, Meredith Giuliani, Fabio Ynoe de Moraes, Geoffrey Liu, Andrew Hope, and Benjamin H. Lok

PURPOSE

Prophylactic cranial irradiation (PCI) is recommended for limited-stage small-cell lung cancer (LS-SCLC) patients with good response to concurrent chemoradiation. We report our institution's 20-year experience with this patient population and associated clinical outcomes.

METHOD

A retrospective cohort of consecutive LS-SCLC patients treated with curative intent chemoradiation at our institution (1997-2018) was reviewed. Overall survival (OS) was calculated using the Kaplan-Meier method, and significant covariates determined by the Cox proportional hazards model. Covariates predictive of PCI were determined using Fisher's exact test and the Mann-Whitney test. Brain failure risk (BFR) was calculated using the cumulative incidence method treating death as a competing event. Treatment cohorts (historic vs. contemporary) were stratified by the median year of diagnosis (2005).

RESULTS

A total of 369 patients with LS-SCLC were identified, of which 278 patients were notionally PCI eligible. PCI was given to 196 patients (71%). Younger age was associated with PCI utilization ($p < 0.001$). PCI utilization rates did not change between the historic and contemporary treatment era ($p = 0.11$), whereas magnetic resonance imaging (MRI) use at baseline and follow-up became more prevalent in the contemporary era ($p = < 0.001$). On multivariable analysis, PCI utilization was associated with improved OS (HR 1.88, 95% CI 1.32-2.69) and decreased BFR (HR 4.66, 95% CI 2.58-8.40). Patients who had MRI follow-up had a higher incidence of BFR (HR 0.35, 95% CI 0.18-0.66) in multivariable analyses.

CONCLUSION

For LS-SCLC patients at our institution, PCI is more frequently utilized in younger patients, and the utilization rate did not change significantly over the past 20 years. PCI was independently associated with improved OS and lower BFR. Omission of PCI in LS-SCLC patients should not be routinely practiced in the absence of further prospective data.

25 Understanding the Potential Improvements in Neurocognition after Radiation Treatment of Brain Tumours with Proton Therapy

Mariana Petruccelli Araujo, Amy Parent, Michael Holwell, Normand Laperrriere, Barbara-Ann Millar, David B. Shultz, Zhihui Amy Liu, Victor Malkov, Kim Edelstein, Derek S. Tsang

PURPOSE

Radiotherapy (RT) can cause long-term changes in neurocognition that may be irreversible. Proton therapy (PT) is able to reduce the dose to normal brain structures as compared with photon RT, however, the actual clinical and neurocognitive benefit is not well known. We compared clinical photon and research proton plans to estimate the possible benefit of PT in adults with brain tumours previously treated with photon RT.

METHOD

Method: In this in silico dosimetry study, 11 patients who were treated with fractionated photon RT for primary CNS tumours between 2008 and 2013 underwent PT re-planning by a trained proton dosimetrist. A 3 mm PTV margin was used in the photon RT plans. Proton plans were created using robustness to 3 mm of motion and 3% change in the CT calibration curve. The generated proton plans were evaluated and compared to their photon counterparts and dosimetric data to organs-at-risk was collected. Statistical comparisons were done using paired t-tests. Memory outcomes (Hopkins Verbal Learning Test – Revised Delayed Recall, HVL-T-R DR) were predicted using converted equivalent-doses-in-2-Gy-fractions (EQD2) to left, right and bilateral hippocampi (HC) based on a previously published model (Ma et al., doi:10.1016/j.radonc.2017.09.035).

RESULTS

In comparing photon vs proton plans, respectively, there was statistical trends to reduction of the mean dose to the right HC (19.7 vs 14.6 Gy, $p = 0.051$) as well as mean (14.8 vs 9.5 Gy, $p = 0.06$) and D50% (17.4 vs 12.1 Gy, $p = 0.07$) to bilateral HC. There were statistically significant reductions in the mean brain dose (16.5 vs 12.3 Gy, $p = 0.002$) and brain D50% (12.5 vs 0.3 Gy $p = 0.01$). Other structures with significantly reduced doses include the bilateral thalami (12.8 vs 4.9 Gy $p = 0.02$), left and right temporal lobes (17.2 vs 12.4 Gy, $p = 0.006$; 18.7 vs 9.6 Gy, $p = 0.002$, respectively) and right cochlea (12.3 vs 2.8 Gy $p = 0.02$). After conversion to EQD2 and applied to a model for risk of HVL-T-R DR decline, lower doses to the right HC in the proton plans are expected to result in lower risk of memory decline related to the treatment.

CONCLUSION

Proton therapy for adults with brain tumors reduces doses to the brain, right cochlea, bilateral thalami, right and left temporal lobes. This may result in less neurotoxic effects of radiation or decline in memory functions. These hypothesis-generating findings should be validated in prospective, longitudinal studies of neurocognition after PT.

26 Quantification of Radiation-Induced Microvascular Changes Using Optical Coherence Tomography and Dynamic Contrast Enhanced MRI

W. Jeffrey Zabel, Nader Allam, Edward Taylor, I. Alex Vitkin

PURPOSE

Stereotactic body radiation therapy (SBRT) has shown promise in the local control of pancreatic adenocarcinoma (PA) in comparison to conventional radiation therapy (RT). While the precise mechanisms of tumor kill in SBRT is still a topic of much debate, preliminary studies have shown that tumor blood vasculature response plays an increasingly important role. The tumor vascular response could thus hold prognostic information that could inform SBRT treatment adaptations. Development of a non-invasive imaging modality to monitor the tumor vascular network during SBRT could thus allow for inter-fraction treatment modifications. Dynamic contrast enhanced magnetic resonance imaging (DCE-MRI) is a clinically applicable imaging modality that can non-invasively monitor the tumor vasculature. However, the use of DCE-MRI for clinical SBRT vascular response monitoring is hindered by its modest spatial resolution and the lack of 'ground truth' to validate its measurements with. Speckle variance optical coherence tomography (svOCT) can provide such high-resolution (~5-15um) depth-resolved 3D images of tumor vasculature in-vivo. Here we correlate DCE-MRI derived vascular metrics with high-resolution svOCT microvascular maps, to test the effectiveness of DCE-MRI in monitoring the tumor vascular network during SBRT.

METHOD

Human pancreatic cancer cells (BxPC3 cell line) were subcutaneously injected into the dorsal skin folds of 12 immunocompromised NRG mice. An MR-compatible plastic window chamber (WC) was surgically sutured into the dorsal

skin-folds of the mice. Mice were exposed to a clinically relevant SBRT irradiation schedule of 10Gy per fraction with 3 fractions (8 irradiated and 4 control mice). DCE-MRI and svOCT imaging was performed 2 days before irradiation, interfraction (between the first and second fraction), and 4 and 10 days after irradiation.

RESULTS

We have performed initial DCE-MRI and svOCT imaging on selected healthy and tumor-bearing mice. The SBRT response study described above is currently underway. Initial inter-modality comparison analysis has revealed good correlations between the DCE-MRI derived vascular metric, k_{ep} (gadolinium transfer constant from extracellular extravascular space to the intravascular space) and the svOCT-derived vascular volume fraction ($R^2=0.63$). The search for other inter-modality correlative metrics is ongoing, for example exploring the linkages between vessel tortuosity (quantified by svOCT) and MRI's k_{trans} parameter (rate of gadolinium extravasation to the extravascular space). Both may prove to be important in the context of SBRT prognostication, and establishing their interrelationship can supply additional and detailed svOCT-derived information content to the clinically relevant MRI.

CONCLUSION

We are currently performing preclinical longitudinal DCE-MRI and svOCT imaging studies throughout a typical SBRT irradiation schedule. We aim to build upon our initial correlative findings by revealing early (2-5 days after commencement of SBRT) svOCT-validated DCE-MRI biomarkers, potentially informing and enabling adaptive SBRT treatments in the clinic.

27 The Contribution of Inflammasomes in RT-Induced Cell Fate and Anti-Tumour Immunity

Cindy Ha, Shirony Nicholson Puthen Veedu, Shane Harding

PURPOSE

Radiotherapy (RT) is a curative treatment modality for many solid cancers. Immune checkpoint blockade (ICB) alleviates repressive mechanisms on the immune system and in combination with RT leads to systemic anti-tumour effects. Our lab has demonstrated that activation of the cGAS-STING pathway by RT induces inflammatory cytokine production and subsequent stimulation of anti-tumour immunity. We have identified three other proteins that contribute to inflammatory signalling after RT: AIM2 (Absent in Melanoma 2), NLRP3 (NOD-Like Receptor Pyrin Domain-Containing 3), and IFI16 (Interferon Gamma Inducible Protein 16). Each of these proteins form distinct protein complexes called inflammasomes that, like cGAS-STING, sense cytoplasmic DNA. Little is known about how inflammasome signalling may change after RT, or how inflammasomes may influence RT-ICB induced anti-tumour immunity. We hypothesize that RT induces inflammasome signalling to influence specific gene expression and cytokine profiles, in tandem with alterations in cellular fate. This change in cellular fate may impact how systemic anti-tumour immunity occurs.

METHOD

This study will be completed using both in vitro and in vivo systems. Briefly, our in vitro systems will use assays such as western blotting, ELISAs, and RT-qPCRs in various human and murine cell lines to evaluate changes in gene expression and cytokine profiles. Previous in vivo data in our lab has established a syngeneic murine model to study RT-ICB induced systemic anti-tumour immunity, in addition to the contributions of cGAS-STING. Our

future in vivo work will focus on how tumour-intrinsic inflammasome activation impacts RT alone and in combination with ICB.

RESULTS

We will present ongoing work in which we show that disruption of inflammasomes genetically or pharmacologically alters cytokine production post-RT. We also find that rationale manipulation of cell fate can alter the balance of cytokine production post-RT with important implications for how the tumour microenvironment may respond to RT.

CONCLUSION

Together our data implicate inflammasomes in the response of epithelial cells to RT and suggest that manipulating cell fate may be a therapeutic strategy to influence treatment responses, such as anti-tumour immunity, in cancer.

28 Change in ADC as an indicator of Radionecrosis

Gwilliam Matt, Muniz Thiago, Xie Jason, Driscoll Brandon, Butler Marcus, Shultz David, Coolens, Catherine

PURPOSE

To investigate if Apparent Diffusion Coefficient (ADC) can identify radionecrosis (RN) which is a serious potential side-effect to stereotactic radiosurgery (SRS) and can be mistaken for tumour progression on imaging. There is an urgent need to develop tools that distinguish between necrosis, progression, and immunotherapy-induced pseudoprogression.

METHOD

A retrospective study of 74 patients treated for melanoma with ipilimumab (prescription: 4x infusion every 3 weeks) and longitudinal Diffusion-weighted, T1-with-contrast, and FLAIR MRI on a range of clinical systems is being undertaken. The preliminary cohort consists of 27 patients. 5 were excluded as diagnosis to treatment was ≥ 1 year. 8 patients had diffusion-weighted-imaging prior to and after SRS. The SRS to ipilimumab time was +43-170 days (mean 93). SRS prescriptions ranged from 15-21Gy/1-3 fractions according to published protocols. 7 patients were imaged ≤ 20 days prior to SRS, 1 at 118 days, and all at times from 20-200 (mean: 109) days post-SRS. Lesions were contoured by an experienced radiation oncologist. Additional ROIs were derived by contracting originals by 2mm in all directions, thus separating the tumour core from the peritumoral rim. The mean ADC value for each ROI prior to radiosurgery, was compared to its corresponding mean value after to obtain a change in ADC value for each ROI. RN and non-RN groups, identified by an experienced oncologist through examination of clinical reports, were compared with a t-test .

RESULTS

The change in ADC observed in core (peritumoral rim excluded) ROIs from prior to post treatment was significantly different between the RN and non-RN groups ($p=0.047$). This exaggerated a similar, not significant trend, observed when the whole tumour ROIs were examined ($p=0.140$).

CONCLUSION

Increasing ADC in the inner-core may be predictive of RN in this study. Observed differences between the complete ROI and contraction ROIs should be considered in future investigations.

29 Strategic Training in Transdisciplinary Radiation Science for the 21st Century (STARS21): 5-year Prospective Evaluation of an Innovative Curriculum in Radiation Research

Parasvi S. Patel, Shahbano Mustafa, Zhihui A. Liu, Shane M. Harding, Marianne Koritzinsky, C. Anne Koch

PURPOSE

STARS21 is a national research training program that has been designed to provide graduate students, postdoctoral fellows, residents, and clinical fellows the skills essential to conduct translational and transdisciplinary research in radiation medicine and aims to address an unmet need for education in this area. We hypothesize that STARS21 enriches graduate and post-graduate training to enable increased trainee proficiencies that can enhance their overall research competencies. To address this further, we developed a novel evaluation tool.

METHOD

From 2015-2020, trainees completed anonymized evaluations of the STARS21 curriculum that included pre- and post-curriculum questionnaires that rated their level of proficiency on a 5-point scale (1=not at all to 5=extremely) for 7 research components. Data were analyzed separately for new (n=86) and returning (n=39) trainees. Two-sided Wilcoxon signed-rank test was used to compare pre- and post-curriculum scores for each component. A p-value ≤ 0.05 was considered statistically significant.

RESULTS

The overall curriculum evaluation completion rate for all trainees was 89%, and for the pre- and post-curriculum evaluations measuring perceived

changes in research competencies of new and returning trainees, the completion rates were 85% and 90%, respectively. Overall, 92% of the trainees indicated that the breadth and depth of the STARS21 curriculum was just right, and that the curriculum was current and relevant. Each year, 100% of trainees indicated that they would recommend the program to their peers. Both new and returning trainees demonstrated significant increases in proficiency in all measured areas of transdisciplinary radiation medicine (p<0.001), interprofessional collaboration (p<0.001 new, p=0.001 returning), transdisciplinary cancer research (p<0.001), translational cancer research (p<0.001), scientific communication (p<0.001 new, p=0.011 returning), personalized medicine (p<0.001 new, p=0.002 returning), and research commercialization (p<0.001). The largest increases (over 1 point) in proficiency were associated with transdisciplinary radiation medicine and research commercialization for both new and returning trainees.

CONCLUSION

STARS21 trainees value the curriculum and program. Using a novel evaluation tool, increased perceived trainee research competencies attributable to the program were demonstrated for all new and returning trainees. This evaluation tool could be applied to other research training programs or adapted to other education settings.

30 Dynamic Contrast-Enhanced CT and MRI to Evaluate Response in Neuroendocrine Liver Metastases Treated with Everolimus and Radiation

John M. Hudson, Laurent Milot, Colleen Bailey, Chirag Patel, Simron Singh, Victor Rodriguez-Freixinos, David Chan, Julie Hallet, Calvin, Law, Sten Myrehaug

PURPOSE

The optimal method to evaluate response in neuroendocrine liver metastases (NELM) treated with radiotherapy (RT) is unknown; tumor perfusion parameters were measured by dynamic contrast-enhanced CT and MRI (DCE-CT and -MRI) to evaluate changes with treatment and correlate with efficacy in a pilot study combining everolimus with RT for NELM.

METHOD

Fourteen patients with oligoprogressive (< 4) NELM received everolimus (up to a max of 7.5 mg daily) for 28 days prior to, concurrent with, and 14 days following RT. All patients received external-beam RT (30Gy in 10 fractions) or SBRT (up to 60Gy in 3-5 fractions over 1-2 weeks), with the preference for SBRT. Each patient had a DCE-CT and -MRI at baseline (t0), prior to RT (t1) and 7 days after RT (t2). Per lesion response was evaluated by RECIST v1.1. Perfusion parameters of blood flow (BF) and blood volume (BV) by DCE-CT, and the volume transfer constant (Ktrans) and extravascular extracellular space (ve) by DCE-MRI were correlated with the change in size of NELM at the 12-month follow-up (12mo). NELM not treated with RT served as internal controls. Statistics were performed using Wilcoxon Signed-Rank Test and Spearman's coefficient.

RESULTS

Twenty-one and 14 treated NELM were evaluable by DCE-CT and -MRI respectively. Compared to t0, BV by DCE-CT increased at t1 by 11% (-15, +37%) (median (quartiles)), then significantly decreased after RT from t1 to t2 by -20% (-37, +2%) with $p < 0.01$. Compared to t0, BF by DCE-CT decreased at t1 by -7% (-25, +33%) and decreased further after RT from t1 to t2 by -13% (-25, +25%) with $p = 0.35$. Trend of increased BV in internal controls at each time point supports that the effect seen is due to RT. Compared to t1, the decrease in BV by DCE-CT after RT correlated with the max % change in the size of the treated NELM at 12mo ($r_s = -0.45$, $p = 0.04$). ve by DCE-MRI increased between t0 and t1 from 0.25 (0.21, 0.35) to 0.32 (0.21, 0.42), $p = 0.59$ and dropped after RT between t1 to t2 to 0.28 (0.21, 0.32) with $p = 0.02$, whereas ve continued to increase in untreated control data. A similar trend was observed for Ktrans. Conventional ORR was 33%; no progression was seen within 12mo.

CONCLUSION

Changes in DCE-CT and -MRI are observed in patients receiving everolimus and everolimus+RT for NELM, with BV and ve decreasing significantly post-RT. Given the challenges in assessing response in NELM using traditional RECIST in any context, DCE-CT and -MRI appear to be promising modalities; further studies are required.